Molecular Plant
Research article

CellPress
Partner Journal

The RNA binding protein EHD6 recruits the m^{6}A reader YTH07 and sequesters *OsCOL4* mRNA into phase-separated ribonucleoprotein condensates to promote rice flowering

Song Cui[1,2,6], Peizhe Song[3,6], Chaolong Wang[1], Saihua Chen[1,4], Benyuan Hao[1], Zhuang Xu[1], Liang Cai[1], Xu Chen[3], Shanshan Zhu[2], Xiangchao Gan[1,5], Hui Dong[1], Yuan Hu[1], Liang Zhou[1], Haigang Hou[1], Yunlu Tian[1], Xi Liu[1], Liangming Chen[1], Shijia Liu[1], Ling Jiang[1], Haiyang Wang[2], Guifang Jia[3,*], Shirong Zhou[1,*] and Jianmin Wan[1,2,*]

[1]State Key Laboratory for Crop Genetics & Germplasm Enhancement and Utilization, Zhongshan Biological Breeding Laboratory, National Observation and Research Station of Rice Germplasm Resources, Nanjing Agricultural University, Nanjing 210095, China

[2]State Key Laboratory for Crop Gene Resources and Breeding, Institute of Crop Science, Chinese Academy of Agricultural Sciences, Beijing 100081, China

[3]Synthetic and Functional Biomolecules Center, Beijing National Laboratory for Molecular Sciences, Key Laboratory of Bioorganic Chemistry and Molecular Engineering of Ministry of Education, College of Chemistry and Molecular Engineering, Peking-Tsinghua Center for Life Sciences, Beijing Advanced Center of RNA Biology, Peking University, Beijing, China

[4]Jiangsu Key Laboratory of Crop Genomics and Molecular Breeding, Agricultural College of Yangzhou University, Yangzhou 225009, China

[5]Max Planck Institute for Plant Breeding Research, Carl-von-Linné-Weg 10, 50829 Köln, Germany

[6]These authors contributed equally to this article.

***Correspondence: Guifang Jia (guifangjia@pku.edu.cn), Shirong Zhou (srzhou@njau.edu.cn), Jianmin Wan (wanjm@njau.edu.cn)**

https://doi.org/10.1016/j.molp.2024.05.002

ABSTRACT

***N*^{6}-Methyladenosine (m^{6}A) is one of the most abundant modifications of eukaryotic mRNA, but its comprehensive biological functionality remains further exploration. In this study, we identified and characterized a new flowering-promoting gene, *EARLY HEADING DATE6* (*EHD6*), in rice. *EHD6* encodes an RNA recognition motif (RRM)-containing RNA binding protein that is localized in the non-membranous cytoplasm ribonucleoprotein (RNP) granules and can bind both m^{6}A-modified RNA and unmodified RNA indiscriminately. We found that EHD6 can physically interact with YTH07, a YTH (YT521-B homology) domain-containing m^{6}A reader. We showed that their interaction enhances the binding of an m^{6}A-modified RNA and triggers relocation of a portion of YTH07 from the cytoplasm into RNP granules through phase-separated condensation. Within these condensates, the mRNA of a rice flowering repressor, *CONSTANS-like 4* (*OsCOL4*), becomes sequestered, leading to a reduction in its protein abundance and thus accelerated flowering through the *Early heading date 1* pathway. Taken together, these results not only shed new light on the molecular mechanism of efficient m^{6}A recognition by the collaboration between an RNA binding protein and YTH family m^{6}A reader, but also uncover the potential for m^{6}A-mediated translation regulation through phase-separated ribonucleoprotein condensation in rice.**

Key words: *N*^{6}-methyladenosine, m^{6}A, EHD6, YTH domain-containing protein, phase separation, heading date

Cui S., Song P., Wang C., Chen S., Hao B., Xu Z., Cai L., Chen X., Zhu S., Gan X., Dong H., Hu Y., Zhou L., Hou H., Tian Y., Liu X., Chen L., Liu S., Jiang L., Wang H., Jia G., Zhou S., and Wan J. (2024). The RNA binding protein EHD6 recruits the m^{6}A reader YTH07 and sequesters *OsCOL4* mRNA into phase-separated ribonucleoprotein condensates to promote rice flowering. Mol. Plant. **17**, 935–954.

INTRODUCTION

Food security is a major challenge for humankind as the world population rapidly increases (Lucas et al., 2021). Rice is one of

Published by the Molecular Plant Shanghai Editorial Office in association with Cell Press, an imprint of Elsevier Inc., on behalf of CSPB and CEMPS, CAS.

the most important cereal crops, feeding more than half of the world population (Foley et al., 2011). Heading date in rice (also known as flowering time), a central link in plant development and reproduction, is a key agronomic landmark that defines regional and seasonal adaptation (Srikanth and Schmid, 2011; Tsuji et al., 2011). Global warming and natural disasters make it particularly vital to breed varieties that are resilient to environmental fluctuations and the adverse effects of climate change.

Numerous rice genes controlling heading date have been cloned, and they can be roughly grouped into two signaling pathways. One is the evolutionarily conserved *OsGI-Hd1-Hd3a* (*rice GIGATEA-Heading date 1-Heading date 3a*) pathway, which is homologous with the *GI-CO-FT* (*GIGATEA-CONSTANS-FLOWERING LOCUS T*) pathway in *Arabidopsis* (Yano et al., 2000; Kojima et al., 2002). The other is the *Ehd1* (*Early heading date1*)-centered monocot-specific pathway (Doi et al., 2004). Both pathways are finally integrated to regulate the production of florigen, a mobile signal that is produced in the leaf but then moves to the shoot apical meristem, where it activates flowering (Taoka et al., 2011; Kobayashi et al., 2012; Lu et al., 2012; Tsuji et al., 2013). Rice has two florigen genes, *Heading date 3a* (*Hd3a*) and *RICE FLOWERING LOCUS T 1* (*RFT1*) (Tamaki et al., 2007; Komiya et al., 2009). *Ehd1*, which encodes a B-type response regulator, promotes flowering by activating the expression of *Hd3a* and *RFT1* under both long-day (LD) and short-day (SD) conditions. *Ehd1* is a flowering integrator, and its expression can be upregulated by *Early Heading Date 2* (*Ehd2*, also known as *RID1* or *OsId1*) (Matsubara et al., 2008), *Early Heading Date 3* (*Ehd3*) (Matsubara et al., 2011), *Early Heading Date 4* (*Ehd4*) (Gao et al., 2013), *Days to Heading 3* (*DTH3*, also known as *OsSOC1* and *OsMADS50*) (Bian et al., 2011), *OsMADS51* (Kim et al., 2007), and others, but downregulated by another group of genes, including *Grain Number*, *Plant Height and Heading Date7* (*Ghd7*) (Xue et al., 2008), *Days to Heading 7* (*DTH7*, also known as *Hd2*) (Gao et al., 2014), *Days to Heading 8* (*DTH8*) (Wei et al., 2010), and *CONSTANS-like 4* (*OsCOL4*) (Lee et al., 2010). *Hd1* encodes an ortholog of the *Arabidopsis* CONSTANS protein, which has two functions, i.e., it promotes flowering under SDs by activating *Hd3a* expression and inhibits flowering by interacting with Ghd7 and repressing *Ehd1* expression under LDs (Yano et al., 2000; Nemoto et al., 2016). However, it is unclear whether there are post-transcriptional RNA modifications involved in controlling heading date.

N^6-Methyladenosine (m^{6}A) is one of the most abundant modifications of eukaryotic mRNAs, and it plays regulatory roles in RNA metabolism (Meyer et al., 2012). The effectors in m^{6}A pathways include a "writer" to catalyze formation of m^{6}A, an "eraser" to remove m^{6}A from the methylated RNA molecules, and a "reader" to exert regulatory functions through selective binding of m^{6}A. The YTH (YT521-B homology) domain-containing proteins are recognized as conserved m^{6}A readers that specifically recognize m^{6}A versus adenosine (A); these proteins include the human YTH domain-containing family proteins 1 to 3 (YTHDF1–3) and YTH domain-containing 1 to 2 (YTHDC1–2) (Shi et al., 2017; Liao et al., 2018; Patil et al., 2018; Liu et al., 2020). The *Arabidopsis* EVOLUTIONARILY CONSERVED C-TERMINUS (ECT) proteins are orthologs of human YTH domain-containing m^{6}A readers; ECT2/3/4 act redundantly in leaf formation, and they are also important for correct root, flower, and fruit formation (Arribas-Hernández et al., 2018, 2020; Scutenaire et al., 2018; Wei et al., 2018). CPSF30-L is another YTH domain-containing m^{6}A reader that regulates flowering time and ABA sensitivity in *Arabidopsis* (Song et al., 2021). However, it is unclear whether there are additional components critical for the decoding of m^{6}A modifications.

In addition, m^{6}A has been shown to functionally modulate mRNA stability (Li et al., 2014; Cao et al., 2016; Du et al., 2016; Roundtree et al., 2017; Zhao et al., 2017), and a few reports suggested that m^{6}A also promotes translation (Li et al., 2017; Liu et al., 2020) and influences alternative splicing (Kasowitz et al., 2018). Interestingly, there are several pieces of evidence suggesting that m^{6}A is also involved in inhibiting translation. For example, a comparison of the translation efficiency between mRNAs modified by m^{6}A and mRNAs lacking m^{6}A (*Mettl14*-knockout cells) revealed that transcripts containing more m^{6}A sites have significantly lower translation efficiency (Ries et al., 2019). This reduction of translation efficiency is attributed to the formation of phase-separated YTHDF-m^{6}A-mRNA complexes, which then partition into phase-separated structures (Ries et al., 2019). Recently, a single-base m^{6}A stoichiometry study found that mRNAs with m^{6}A have a lower translation efficiency than mRNAs without m^{6}A (Liu et al., 2023), which provides additional evidence of the role of m^{6}A in translation repression. Moreover, a genome-wide correlation analysis between m^{6}A modification and translation in human cells found that nearly half of m^{6}A modifications have a negative impact on translation efficiency, suggesting that m^{6}A can also suppress translation in addition to its previously recognized translation-promoting function (Zhang et al., 2020). It is hypothesized that whether m^{6}A enhances or suppresses the translation efficiency depends on the binding of specific RNA binding proteins (RBPs) (Zhang et al., 2020). However, direct biochemical and genetic evidence for the translation repression effect of m^{6}A is still lacking. Besides, the molecular mechanism for m^{6}A modification-mediated translation repression is largely unknown.

In this study, we found an RRM domain-containing RBP named EARLY HEADING DATE 6 (EHD6) that regulates heading date in rice independently of light and temperature conditions. We demonstrate that EHD6 localizes to the non-membranous cytoplasm ribonucleoprotein (RNP) granules and can bind both m^{6}A and A indiscriminately. However, EHD6 directly interacts with YT521-B homology 07 (YTH07), an YTH domain-containing m^{6}A reader, and this interaction not only endows EHD6-YTH07 with strong affinity to m^{6}A targets but also triggers partial relocation of YTH07 from the cytoplasm to RNP granules through phase-separated condensation. The condensation sequesters the mRNA of a flowering repressor, *OsCOL4*, leading to a reduction in OsCOL4 protein accumulation and promoting flowering via the *Ehd1* pathway. Our results not only demonstrate the effect of the interaction between an RBP and YTH family m^{6}A reader on the efficiency of m^{6}A binding but also uncover a molecular mechanism for m^{6}A modification-mediated repression of protein accumulation in rice.

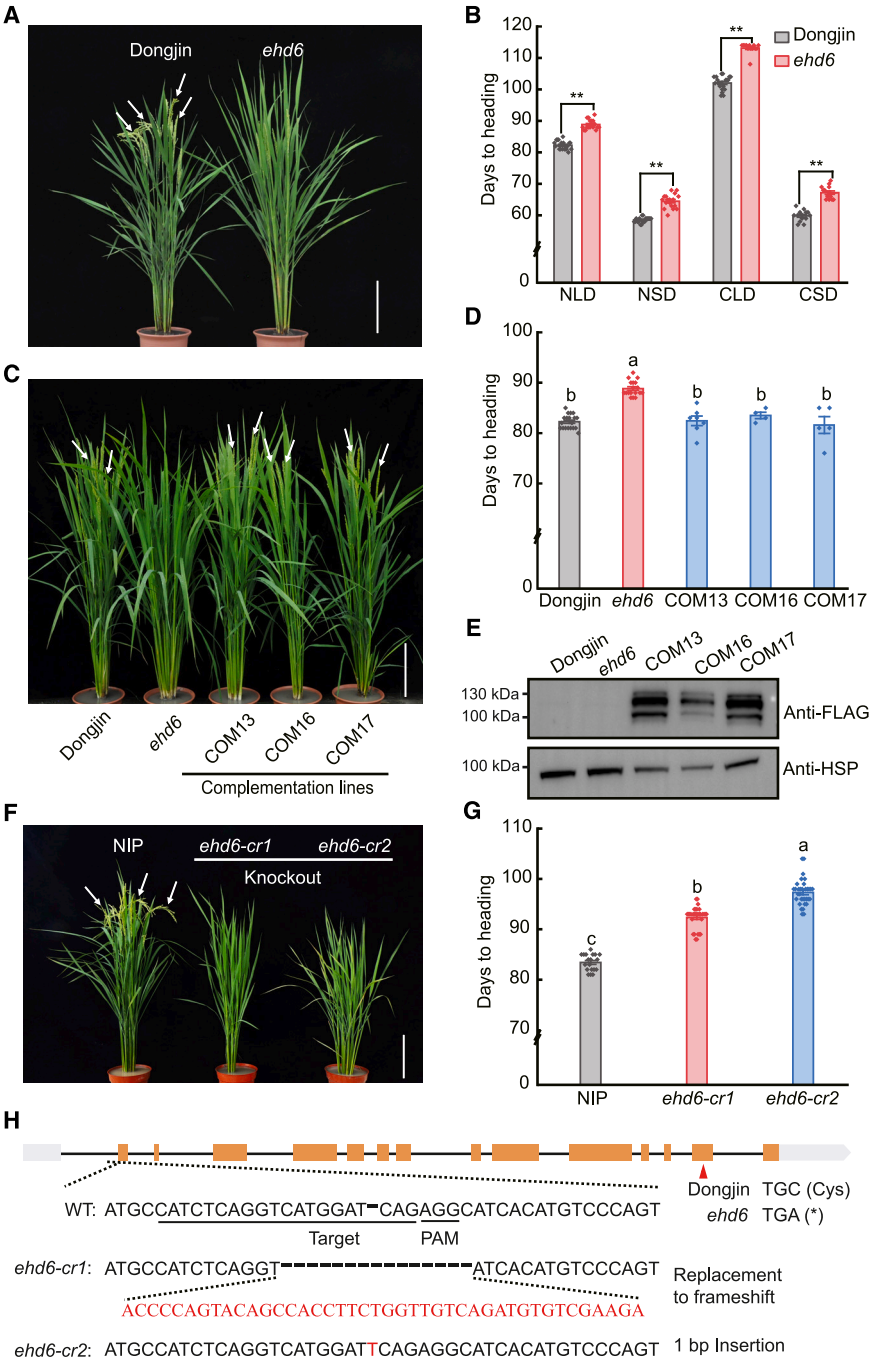

Figure 1. Characterization of the late flowering *ehd6* mutant.

(A) Phenotypes of Dongjin and the *ehd6* mutant at the bolting stage under natural long-day (NLD) conditions. Scale bar corresponds to 20 cm. White arrows indicate rice panicles.

(B) Heading dates of Dongjin and the *ehd6* mutant under NLD, natural short-day (NSD), controlled long-day (CLD) (14 h light/10 h dark), and controlled short-day (CSD) (10 h light/14 h dark) conditions. Values are means ± SD; n >10. $^{**}P$ <0.01; Student's t-tests.

(C and D) Phenotypes and heading dates of Dongjin, the *ehd6* mutant, and *pEHD6:EHD6-FLAG/ehd6* transgenic lines. COM13, COM16, and COM17 are three independent lines showing flowering phenotype complementation. Scale bar corresponds to 20 cm. White arrows indicate rice panicles. Values are means ± SD; n > 4. Different letters denote significant difference determined by one-way analysis of variance (P < 0.05).

(E) Western-blot detection of the EHD6 protein in Dongjin, the *ehd6* mutant, and complementation lines. Anti-FLAG antibody was used. Heat shock protein 90 (HSP) was used as the loading control.

(F and G) Phenotypes and heading dates of Nipponbare (NIP) and two CRISPR-Cas9 knockout lines. *ehd6-cr1* and *ehd6-cr2* are independent edited lines. Scale bar corresponds to 20 cm. White arrows indicate rice panicles. Values are means ± SD; n > 10. Different letters denote significant difference determined by one-way analysis of variance (P < 0.05).

(H) Gene structure of *EHD6*. Gray boxes represent the untranslated regions, yellow boxes the coding region, and black lines the introns. The positions of the SNP between Dongjin and the *ehd6* mutant and the mutations in two mutants generated by CRISPR-Cas9 are indicated.

RESULTS

Characterization of a late flowering mutant, *ehd6*

We generated a Dongjin (*Oryza sativa* ssp. *japonica*) mutant population using tissue culture-mediated mutagenesis to identify novel genes involved in flowering regulation. A late flowering mutant, named *early heading date 6* (*ehd6*), was identified. The mutant flowered 88.8 ± 1.5 days after sowing, about 1 week later than the wild type (82.3 ± 1.4), under natural long-day (NLD) conditions at Nanjing (31°14′N, 118°22′E), and it also flowered approximately a week later under natural short-day (NSD) conditions at Lingshui (18°22′N, 109°45′E) (Figure 1A and 1B and Supplemental Table 1). The late flowering phenotype was verified under both controlled long-day (CLD) and controlled short-day (CSD) conditions (Figure 1B). These results indicated that the late flowering phenotype of the *ehd6* mutant was independent of photoperiodic and temperature conditions. To further test this notion, we planted the *ehd6* mutant and Dongjin at five different latitudes and at two adjacent locations with different altitudes (Supplemental Figure 1A). These latter locations were separated by about 20 km (hence had similar photoperiods) but had an altitude difference of more than 1200 m, resulting in a more than 7°C temperature difference (Supplemental Figure 1B). The *ehd6* mutant was consistently later flowering than Dongjin at all locations (Supplemental Table 1). The mutant produced fewer but larger seeds, and its plant height, thousand grain weight, grain width, and grain length were increased relative to those of Dongjin. There was no difference in tiller number under NLD conditions (Supplemental Figure 1C).

Molecular cloning and expression profile of *EHD6*

F_1 plants derived from a cross between the *ehd6* mutant and Dongjin showed a similar heading date to Dongjin (Supplemental Figure 2A and 2B), and the F_2 population segregated 188 early flowering:66 late flowering ($\chi^2_{3:1}$ = 0.13; P_{1dfq} > 0.05), suggesting that the late flowering phenotype was caused by a single recessive Mendelian factor (Supplemental Figure 2C). We mapped *EHD6* to chromosome 2 using a modified MutMap method (Fekih et al., 2013) (Supplemental Figure 2D). Sequence analysis revealed that the *ehd6* allele has a single-nucleotide substitution (C to A) in the exon of the gene *MEI2-LIKE PROTEIN4* (*OML4*, Os02g0517531), which was reported previously to control grain size and weight (Lyu et al., 2020), creating a stop codon and causing pre-termination of the translational product (Figures 1H and Supplemental Figure 2E). Thus, we predicted *OML4* as the candidate gene for *EHD6*. Transgenic plants carrying the full coding sequence (CDS) of *OML4* driven by the native promoter fully rescued the *ehd6* mutant phenotype (Figure 1C–1E). We also generated two independent *OML4* knockout lines in Nipponbare by CRISPR-Cas9 gene editing (Figure 1H). Both the knockout lines flowered later than Nipponbare (Figure 1F and 1G). We concluded that *OML4* corresponds to *EHD6*.

To investigate the spatial and temporal transcription patterns of *EHD6*, we examined the expression levels of *EHD6* in various tissues and at different growth stages. Quantitative reverse-transcriptase PCR (qRT–PCR) analysis revealed that *EHD6* was expressed in all tissues examined, with relatively higher expression in the panicles (Figure 2A). *EHD6* maintained a high expression level under both LD and SD conditions during the entire vegetative growth period (Figure 2B). *EHD6* transcript in leaves began to accumulate around dusk and gradually declined after daybreak under both LD and SD conditions, thus behaving diurnally (Figure 2C and 2D). Moreover, analysis of transgenic plants expressing the GUS (β-glucuronidase) reporter gene driven by the *EHD6 promoter* (*pEHD6*:*GUS*) confirmed the ubiquitous expression pattern of *EHD6* (Supplemental Figure 2F).

EHD6 interacts with the m^{6}A reader YTH07

To investigate how EHD6 regulates flowering, yeast two-hybrid screening was performed to identify EHD6-interacting proteins. YTH07 (Os04g0608800), annotated as a YT521-B-like family protein (homolog of the mammalian YTH family m^{6}A reader), was identified as an EHD6-interacting partner (Figure 2E). The interaction was substantiated through *in vitro* pull-down and bimolecular fluorescence complementation (BiFC) assays (Figure 2F and 2G). Furthermore, co-immunoprecipitation (Co-IP) experiments conducted in *Nicotiana benthamiana* leaf epidermal cells and the protoplasts of stable transgenic rice plants expressing EHD6-FLAG provided further evidence confirming the interaction between EHD6 and YTH07 *in vivo* (Figure 2H and 2I).

We further examined which specific region of YTH07 is responsible for interacting with EHD6. YTH07 was divided into three fragments: the N-fragment containing the PrLD domain, the M-fragment representing the YTH domain, and the remaining fragment referred to as the C-fragment (Supplemental Figure 3A). Through pull-down and BiFC assays, we found that both the N-fragment and M-fragment of YTH07 can interact with EHD6, while the C-fragment cannot (Supplemental Figure 3B and 3C).

To substantiate the biological relevance of the EHD6-YTH07 interaction, we generated the *yth07* knockout lines by CRISPR-Cas9 editing (Supplemental Figure 4A). Two loss-of-function *yth07* mutants both exhibited delayed flowering under NLD and NSD conditions (Figure 3A and 3B), indicating that YTH07 has a floral promoting function just like EHD6.

We also obtained a *ehd6 yth07* double mutant, which flowered slightly later than both the *ehd6* and *yth07* single mutants under both NLD and NSD conditions; notably the phenotype of *ehd6 yth07* was closer to that of *ehd6*, especially under NLD conditions (Figure 3C and 3D). These observations suggest a genetic interaction between EHD6 and YTH07.

EHD6 can bind the m^{6}A-modified RNAs

EHD6 was annotated as an RRM domain-containing RBP (Supplemental Figure 7B), and its interaction partner, YTH07, contains a YTH domain (Supplemental Figure 3A), which is an evolutionarily conserved m^{6}A binding domain (Patil et al., 2018). To assess whether EHD6 exhibits affinity for m^{6}A similar to YTH07, we conducted an RNA electrophoretic mobility shift assay (EMSA) utilizing purified recombinant EHD6 and YTH07 proteins along with RNA oligos. We synthesized an m^{6}A-containing RNA oligo as a probe (m^{6}A probe), and another oligo with the same sequence but with m^{6}A replaced by A (A probe) was used as a control (Supplemental Table 2). The results showed that EHD6 could bind both the m^{6}A probe and A probe (Figure 4A), while YTH07 specifically bound m^{6}A through the YTH domain (Figure 4B and Supplemental Figure 5A). To further investigate the relationship between EHD6 and m^{6}A *in vivo*, we performed RNA immunoprecipitation (RIP) followed by liquid chromatography-tandem mass spectrometry (LC–MS/MS) detection using *pEHD6*:*EHD6-FLAG*/*ehd6* transgenic plants. LC–MS/MS results showed that more m^{6}A-modified RNAs were pulled down by EHD6-FLAG compared with control immunoglobulin G (IgG) (Figure 4C). These findings suggest a close association between EHD6 and m^{6}A.

EHD6 efficiently recognizes the m^{6}A modification in collaboration with YTH07

To elucidate the relationship between EHD6, YTH07, and m^{6}A modification at the whole-transcriptome level, we employed formaldehyde crossing-linking and immunoprecipitation (FA-CLIP) to identify mRNAs associated with EHD6 and YTH07. The assays were separately conducted using transgenic plants expressing EHD6-FLAG (*pEHD6*:*EHD6-FLAG*) and YTH07-GFP (*pYTH07*:*YTH07-GFP*) fusion proteins. Two biological replicates of EHD6-CLIP analysis uncovered 9872 peaks corresponding to 7263 genes, while the YTH07-CLIP experiment, replicated biologically twice, revealed 2009 peaks corresponding to 1751 genes (Supplemental Figure 5B).

Furthermore, we performed a combined analysis of the published m^{6}A-SEAL-seq data (Wang et al., 2020b) and the EHD6-CLIP and

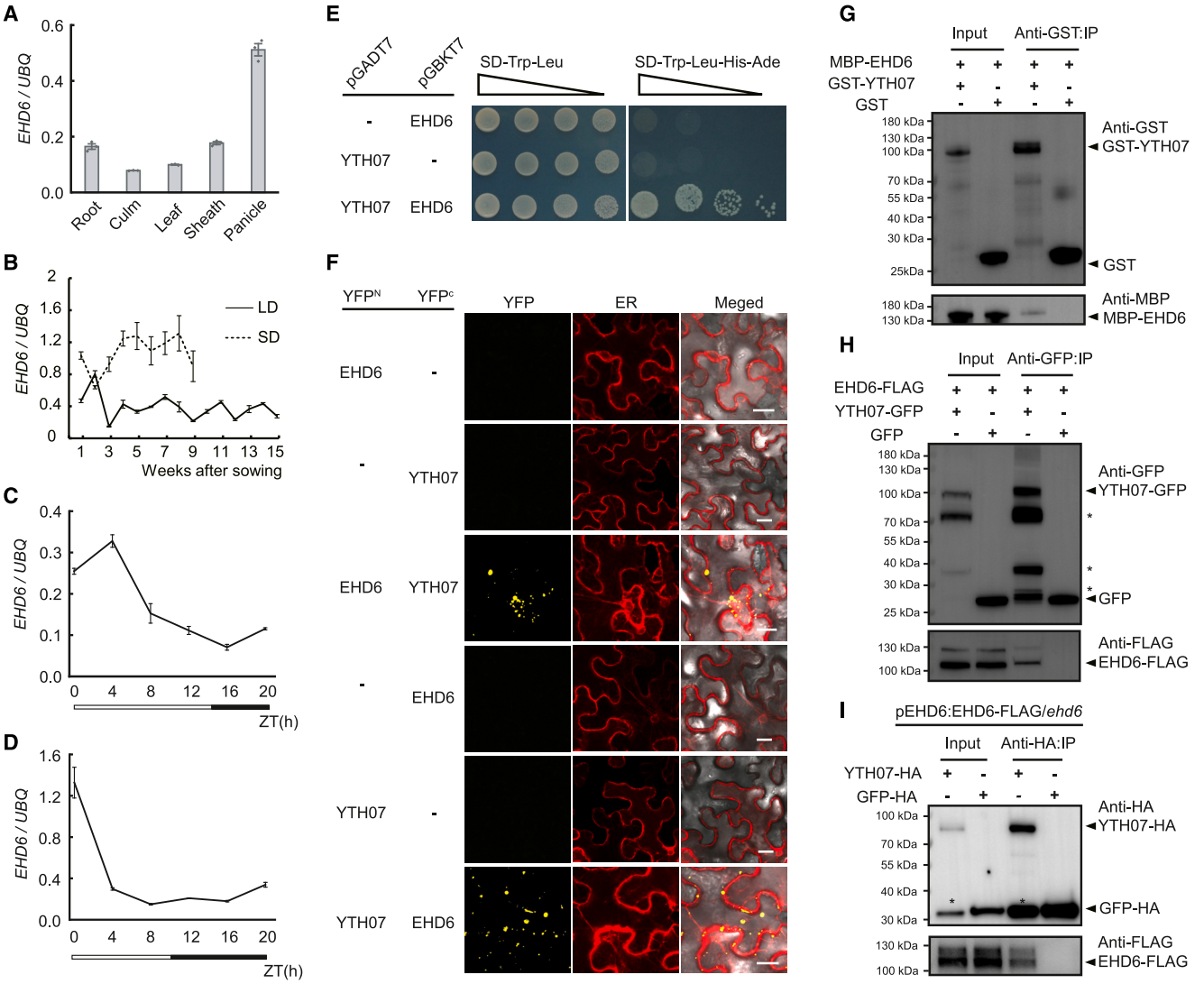

Figure 2. Expression profile of EHD6 and its interaction with YTH07.

(A) qRT–PCR analysis of *EHD6* in different tissues. Tissues from Dongjin were collected from roots, culms, leaves, leaf sheaths, and panicles.

(B) Expression of *EHD6* in CLD and CSD conditions (assessed weekly from sowing until flowering).

(C and D) Rhythmic expression of *EHD6* under CLD **(C)** and CSD **(D)** conditions. White and black boxes denote periods of light and darkness, respectively. The rice *UBIQUITIN* gene was used as the internal control, and values are means ± SD (n = 3) in **(A)–(D)**.

(E) Yeast two-hybrid assays showing that EHD6 interacts with YTH07. Transformed yeast cells were grown on DDO (SD/-Trp/-Leu) and QDO (SD/-Trp/-Leu/-His/-Ade) plates.

(F) Bimolecular fluorescence complementation (BiFC) assays showing that EHD6 interacts with YTH07 in *N. benthamiana* leaf epidermal cells. Scale bar corresponds to 25 μm. ER denotes the endoplasmic reticulum.

(G) An *in vitro* pull-down assay validated the direct interaction between EHD6 and YTH07. "–" and "+" represent absence and presence of the corresponding proteins.

(H) An *in vivo* Co-IP assay verified the interaction between EHD6 and YTH07 in *N. benthamiana* leaf epidermal cells. "–" and "+" represent absence and presence of the corresponding proteins. * represents truncated YTH07-GFP fragments.

(I) A Co-IP experiment using protoplasts from the EHD6-FLAG complementation lines revealed the interaction between EHD6 and YTH07. "–" and "+" represent absence and presence of the corresponding proteins. * represents truncated YTH07-HA fragments.

YTH07-CLIP data, and found that 69% (966 out of 1397) of the genes associated with both EHD6-CLIP and YTH07-CLIP overlapped with m^{6}A-modified genes, which predominantly encode mRNAs (Figure 4D and Supplemental Figure5C, and Supplemental Table 3). This set of genes, termed EHD6/YTH07/m^{6}A targets, was selected for further analysis. Clustering all EHD6/YTH07/m^{6}A targets sites in HOMER (hypergeometric optimization of motif enrichment) uncovered strongly enriched motifs, YUGUA and UGUAD, for EHD6 and YTH07, respectively (Supplemental Figure 5D). These motifs resembled the canonical m^{6}A motif URUAH (Y = C/U, D = A/G/U, R = A/G, H = A/C/U) in plants (Zhou et al., 2022). The EHD6/YTH07/m^{6}A targets exhibited enriched EHD6 and YTH07 binding peaks closely associated with the m^{6}A site (Figure 4E). This finding suggested that EHD6 is also highly associated with m^{6}A just like its interaction partner YTH07.

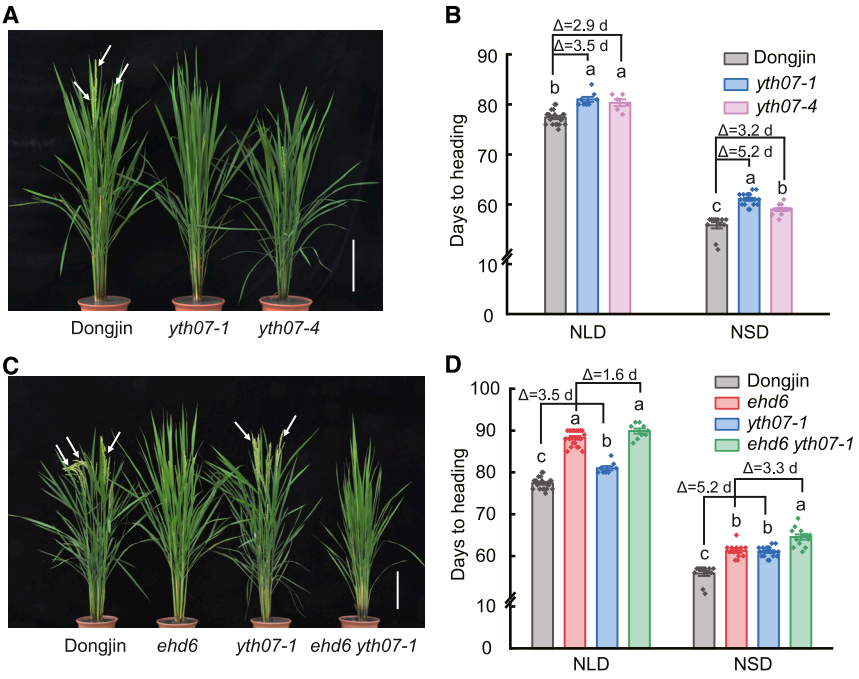

Figure 3. YTH07 participates in promoting rice flowering.

(A) Phenotype of Dongjin and two *yth07* knockout lines at the bolting stage under NLD conditions. Scale bar corresponds to 20 cm. White arrows indicate rice panicles. *yth07-1* and *yth07-4* are independent edited lines.

(B) Heading dates of Dongjin and two *yth07* knockout lines under NLD and NSD conditions. Values are means ± SD; $n > 5$. Δ represents the heading date difference between the two lines.

(C) Phenotypes of Dongjin and the *ehd6* , *yth07-1*, and *ehd6 yth07* mutant lines at the bolting stage under NLD conditions. Scale bar corresponds to 20 cm. White arrows indicate rice panicles.

(D) Heading dates of Dongjin and the *ehd6*, *yth07-1*, and *ehd6 yth07* mutant lines at the bolting stage under NLD conditions and NSD conditions. Values are means ± SD; $n > 7$. Δ represents the heading date difference between the two lines. Different letters denote significant difference determined by one-way analysis of variance ($P < 0.05$).

Considering that EHD6 is an RBP and interacts with YTH07, we tested whether or not the binding of YTH07 to m^{6}A is associated with its interaction partner. To this end, we categorized YTH07 and m^{6}A binding targets into EHD6-marked (termed EHD6(+)/YTH07/m^{6}A targets) and non-EHD6-marked (termed EHD6(−)/YTH07/m^{6}A targets) subgroups. The results showed that YTH07 exhibits a stronger binding affinity for m^{6}A-enriched transcripts when EHD6 is present (Figure 4F). To further explore the significance of the interaction between EHD6 and YTH07 for m^{6}A binding, we performed additional EMSA assays. Interestingly, both YTH07 and EHD6 individually showed relatively low m^{6}A affinity. However, the affinity for the m^{6}A probe increased substantially in the presence of both YTH07 and EHD6 (Figure 4G and Supplemental Figure 5E). Notably, this enhancement did not occur when the m^{6}A probe was substituted with an A probe (Figure 4H). These results suggested the cooperative role of EHD6 and YTH07 in m^{6}A recognition.

To further confirm this *in planta*, we transiently expressed equal amounts of the *YTH07-GFP* construct in protoplasts of Dongjin and *ehd6*. GFP RIP followed by an LC–MS/MS assay showed that significantly more m^{6}A-modified RNAs were pulled down by YTH07-GFP in Dongjin than in *ehd6* (Figure 4I). Conversely, we observed no significant difference in the amount of m^{6}A-modified RNAs pulled down by EHD6-FLAG when equal amounts of the *EHD6-FLAG* construct were introduced into the protoplasts of Dongjin and *yth07* (Supplemental Figure 5F). These results suggested a supportive role of EHD6 in the binding of YTH07 to m^{6}A, but not vice versa. Phylogenetic analysis revealed 12 YTH domain-containing proteins in the rice genome (Supplemental Figure 6A). Pull-down and BiFC assays demonstrated that EHD6 can interact with most other YTH family members (YTH08 and YTH09 were not tested, as they could not be amplified by PCR) (Supplemental Figure 6B–6F). The lower dependency of EHD6 on YTH07 is likely due to redundancy within the YTH family. In summary, EHD6 cooperates with YTH07 for efficient m^{6}A recognition.

EHD6 is present in granule-like condensates in the cytoplasm

To investigate the subcellular location of EHD6, we generated *pEHD6:EHD6-GFP/ehd6* transgenic lines. The GFP fluorescence was visible as scattered foci in the cytoplasm of rice root cells, with no observed GFP signals in the nucleus (Figure 5A). To confirm the cytoplasm localization of EHD6, we isolated the nuclear and cytoplasmic proteins from the leaves of a *pEHD6:EHD6-FLAG/ehd6* transgenic complementation line; in an immunoblot experiment the EHD6 protein was detected only in the cytoplasm (Supplemental Figure 7A). Upon analyzing the protein sequence of EHD6, we discovered that, in addition to RRM domains, it also contains a PrLD domain (Supplemental Figure 7B). This domain has the potential to undergo phase separation (Fang et al., 2019; Wang et al., 2020a). To confirm whether the condensation of EHD6 was a consequence of phase separation, we conducted a fluorescence recovery after photobleaching (FRAP) assay. The results showed that EHD6-GFP fluorescence gradually redistributed from the unbleached area to the bleached area (Figure 5B and 5C). In addition, the fluorescent spots could fuse to form larger spots (Supplemental Video 1), which is a phenomenon typical of phase separation. The scattered foci within the cytoplasm resembled non-membrane-enclosed RNP granules such as processing bodies (P-bodies) and stress granules (SGs), which dynamically form through the phase separation of RNAs and proteins (Xu et al., 2006; Weber et al., 2008; Erickson et al., 2011; Ivanov et al., 2019; Youn et al., 2019; Ripin et al., 2023). Subsequently, we constructed an *EHD6-GFP* fusion construct and transiently expressed it in rice protoplasts

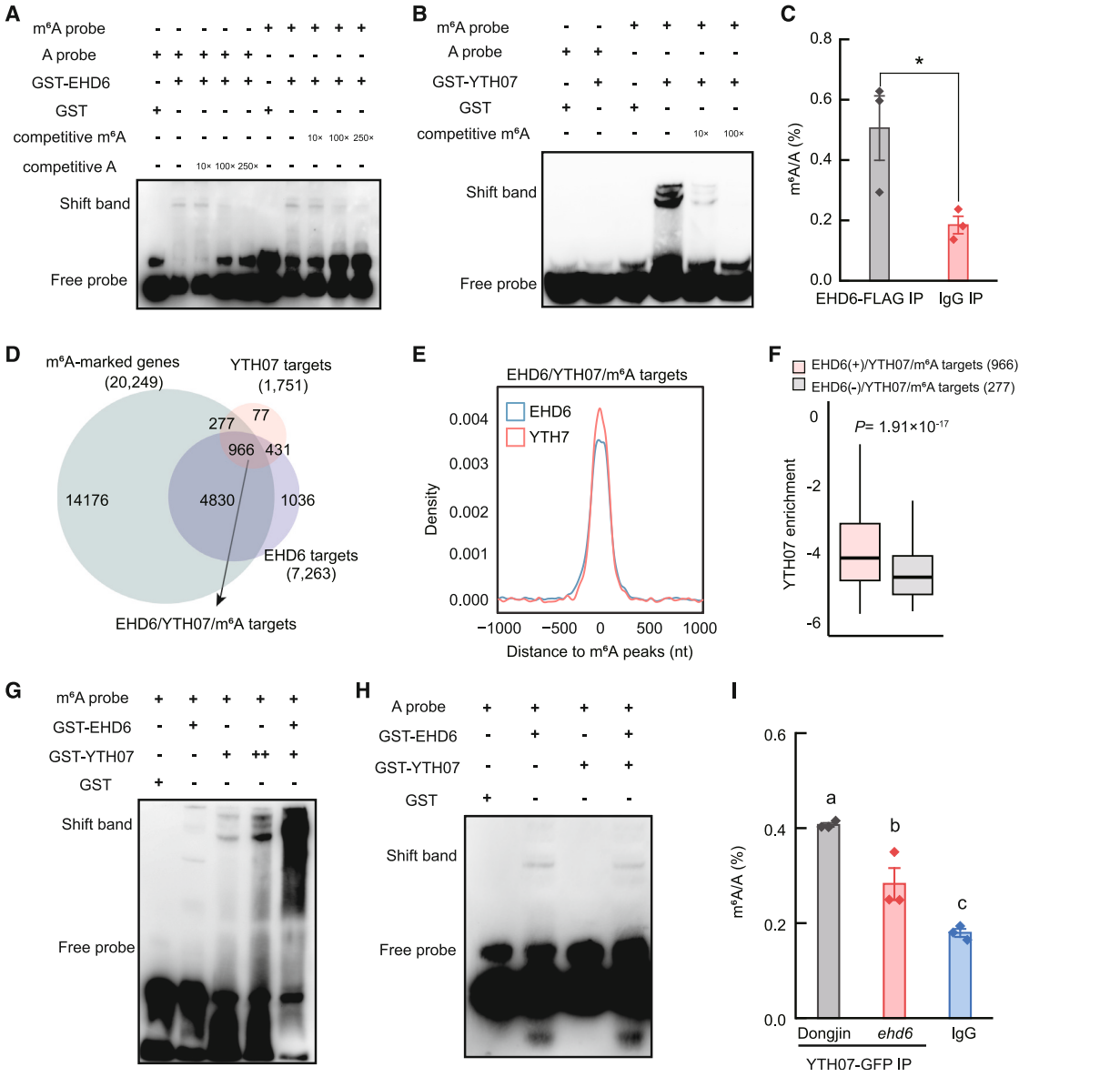

Figure 4. EHD6 shows strong m^{6}A binding affinity in collaboration with YTH07.

(A) EMSA assays show that EHD6 binds both unmethylated RNA and m^{6}A-modified RNA. The unmethylated RNA (A probe) and m^{6}A-modified RNA (m^{6}A probe) were biotin-labeled fragments: 5′-bio-GUGCCCAACGCCCAAAAAXCACAGCCAAXCUCCGCGAGAAXCCGAGCUGC-3′, where X = A or m^{6}A. The competitive A/m^{6}A probes have the same sequence as the A/m^{6}A probes but without the biotin label.

(B) EMSA assay shows that YTH07 binds m^{6}A-modified RNA but not unmethylated RNA.

(C) *In vivo* FA-RIP-LC–MS/MS showing that m^{6}A is enriched in EHD6-FLAG-bound RNA. Data are presented as means ± SD, $n = 3$. * denotes significant difference determined by Student's *t*-tests ($P < 0.05$).

(D) Overlap of the identified genes encoding EHD6 binding, YTH07 binding, and m^{6}A-modified RNAs (termed EHD6/YTH07/m^{6}A targets).

(E) Density plots showing the distance from the EHD6 or YTH07 binding site within the EHD6/YTH07/m^{6}A targets to the m^{6}A site.

(F) Box blot showing the enrichment of YTH07 targets with m^{6}A modifications when EHD6 is present or absent. *P* value was calculated by Student's *t*-tests.

(G) EMSA assays show that EHD6-YTH07 has stronger m^{6}A affinity compared with YTH07 or EHD6 individually.

(H) EMSA assays show that interaction of EHD6 and YTH07 does not influence binding to unmethylated RNA. The final concentrations of proteins and probes used in the EMSA assays are as follows: GST-EHD6, 900 nM; GST-YTH07, 60 nM; RNA oligo, 2 nM.

(I) *In vivo* FA-RIP-LC–MS/MS showing that EHD6-YTH07 binds more m^{6}A than YTH07 alone. Values are means ± SD, $n = 3$. Different letters denote significant difference determined by one-way analysis of variance ($P < 0.05$).

and *N. benthamiana* leaf epidermal cells to compare the subcellular localization of the EHD6 protein with that of RNP granule markers. EHD6-GFP did not merge with the P-body marker AtDCP1-mCherry (Iwasaki et al., 2007), but it perfectly merged with the SG marker AtPAB2-mCherry (Scutenaire et al., 2018) (Supplemental Figure 7C–7E).

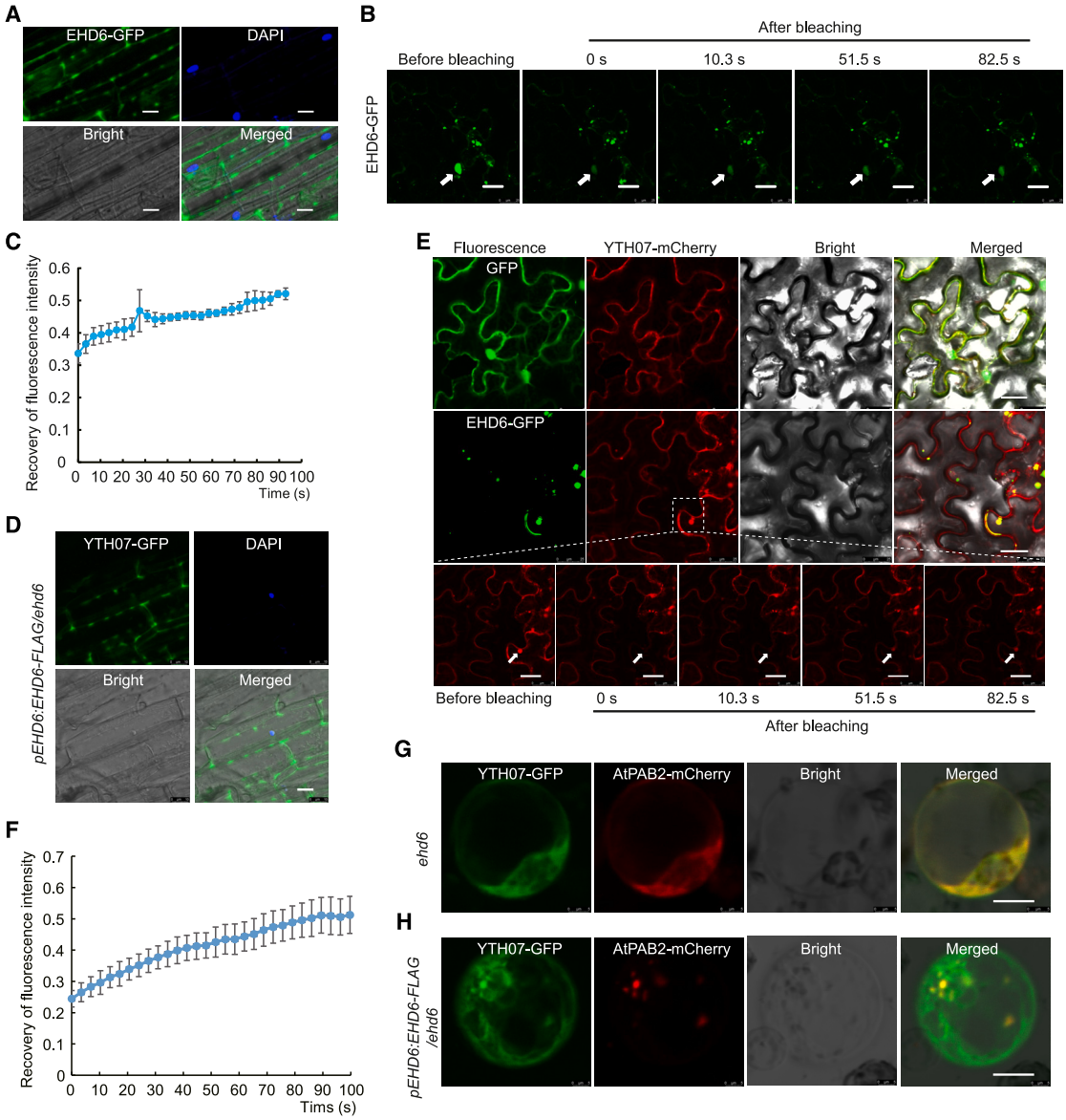

Figure 5. EHD6 localizes and recruits YTH07 to RNP granules through phase separation.

(A) Subcellular localization of the EHD6-GFP fusion protein in *pEHD6*:*EHD6-GFP*/*ehd6* transgenic plant root cells. DAPI staining was used to mark nuclei. Scale bar corresponds to 8 μm.

(B) Fluorescence recovery after photobleaching (FRAP) of the EHD6 protein in *N. benthamiana* leaves; bleaching is indicated by white arrows. Scale bars correspond to 5 μm.

(C) Fluorescence recovery curve averaged for granules from three cells after normalization and correction for bleaching depth. Data are means ± SD, $n = 3$.

(D) Subcellular localization of the native promoter-driven YTH07-GFP (*pYTH07*:*YTH07-GFP*) fusion protein in the root cells of transgenic plants. The EHD6 transgenic complementation line (*pEHD6:EHD6-FLAG*/*ehd6*) was utilized as the transgenic recipient. DAPI staining was used to mark nuclei. Scale bar corresponds to 10 μm.

(E) YTH07 is diffusely localized in the cytoplasm when co-expressed with GFP alone in tobacco leaf cells. However, when co-expressed with EHD6-GFP, YTH07 partially relocates to RNP granules. FRAP assay suggests that the RNP granule localization of YTH07 is produced through phase separation. The upper images show co-location of EHD6-GFP and YTH07-mCherry before laser bleaching, and the lower images show the state of fluorescence recovery at different time points. The bleaching area is indicated by white arrows. Scale bar corresponds to 25 μm.

(F) Fluorescence recovery curve averaged for YTH07-mCherry granules from three cells after normalization and correction for bleaching depth. Data are means ± SD, $n = 3$.

(G and H) Subcellular localization of YTH07-GFP in protoplasts of *ehd6* and the EHD6 transgenic complementation line (*pEHD6*:*EHD6-FLAG*/*ehd6*). Scale bar corresponds to 10 μm.

SGs are known to form in response to stress (Kosmacz et al., 2019), and the reported SG-localized proteins display punctate foci only when stress occurs to stall translation initiation but allow elongation to occur after the stress is removed (Ivanov et al., 2019; Youn et al., 2019). However, our observations suggest that EHD6 tends to condense even under normal conditions (Figure 5A and Supplemental Figure 7C–7E). To exclude potential stress during our observations, we used a previously reported SG-localized m^{6}A reader, ECT2, as a control (Scutenaire et al., 2018). As expected, ECT2 localized in the cytoplasm under normal temperatures but relocated to SGs under high temperatures, similar to the SG marker AtPAB2-mCherry (Supplemental Figure 7F). However, EHD6 formed condensates in the cytosol under both normal and high-temperature conditions (Supplemental Figure 7F). These results suggested that the SG-like location of EHD6 is independent of stress stimulation; we would rather call it an RNP granule-localized protein.

The PrLD domain is vital for the condensation of EHD6

To investigate whether the condensation of EHD6 is related to the PrLD domain or another RRM domain, we generated three truncated EHD6 proteins: EHD6-ΔN-RRM lacking the two N-terminal RRM domains, EHD6-ΔPrLD lacking the PrLD domain, and EHD6-ΔC-RRM lacking the C-terminal RRM domain (Supplemental Figure 8A). Subsequently, these truncated proteins were fused with GFP and introduced into tobacco epidermal cells. Notably, we observed that the condensation of EHD6 was abolished only when the PrLD domain was absent (Supplemental Figure 8A). Furthermore, FRAP assays conducted on EHD6-ΔN-RRM (Supplemental Figure 8B, 8D, and 8F) and EHD6-ΔC-RRM truncations (Supplemental Figure 8C, 8E, and 8G) indicated that lack of either the N-terminal or the C-terminal RRM domain did not significantly affect fluorescence recovery, thereby establishing the indispensability of the PrLD domain for phase separation.

EHD6 recruits YTH07 to RNP granules through phase separation

We also investigated the subcellular localization of YTH07. The YTH07-GFP fusion protein, driven by its native promoter, displayed a scattered focal distribution in EHD6-complemented transgenic rice root cells (Figure 5D). To explore whether the condensation of YTH07 is related to EHD6, we transiently expressed YTH07-mCherry in *N. benthamiana* leaf epidermal cells. When YTH07-mCherry was expressed alone, it exhibited a diffuse cytoplasm localization pattern (Figure 5E). However, when co-expressed with EHD6, YTH07, together with EHD6, partially formed condensates (Figure 5E and 5F). In addition, YTH07-GFP was diffused throughout the cytoplasm in the protoplasts of the *ehd6* mutant (Figure 5G). However, a fraction of the YTH07-GFP protein formed condensates in the protoplasts of EHD6 complementation line (Figure 5H). All the results indicated that EHD6 recruits YTH07 to RNP granules through phase separation.

Previous studies have shown that m^{6}A promotes YTHDF2-mediated phase separation (Wang et al., 2020a), and our results indicated that EHD6 is associated with m^{6}A. To further confirm whether the RNP-mediated condensation of EHD6 is a product of m^{6}A-triggered phase separation, we conducted an *in vitro* phase separation assay using purified GFP-EHD6 protein and RNA oligos. The probe sequence was the same as that of the A/m^{6}A probe used in the EMSA, but the 5′ biotin modification was replaced with CY5 (Supplemental Table 2). The results showed that, in the presence of m^{6}A, GFP-EHD6 condensed into droplets (Supplemental Figure 7G). However, adding the same amount of purified GFP or replacing m^{6}A with A did not yield similar results (Supplemental Figure 7G). Moreover, increasing the concentration of GFP-EHD6 or introducing YTH07 protein enlarged the GFP-EHD6 condensates (Supplemental Figure 7G). Importantly, CY5-m^{6}A co-localized with the GFP-EHD6 condensates (Supplemental Figure 7G), suggesting that the m^{6}A-modified RNA was included in the condensates. These results suggested that EHD6 is an RNP granule-localized protein and recruits the m^{6}A reader YTH07 to RNP granules through phase separation.

Both EHD6 and YTH07 recognize *OsCOL4* mRNA

A photoperiod-independent heading date gene, *OsCOL4* (Lee et al., 2010), was among the genes encoding EHD6/YTH07/m^{6}A-associated RNAs (Figures 4D and 6A). RIP-qPCR, conducted using EHD6-FLAG and YTH07-GFP transgenic plants, provided evidence supporting the binding of *OsCOL4* mRNA by both EHD6 and YTH07 (Figure 6B and 6C). In addition, detection through m^{6}A-IP-qPCR confirmed the presence of m^{6}A modifications on *OsCOL4* mRNA (Figure 6D).

To probe the interdependence between EHD6 and YTH07 in *OsCOL4* binding, an equal amount of *YTH07-FLAG* construct was introduced into both *yth07* and *ehd6 yth07* protoplasts. Subsequently, we assessed the enrichment of *OsCOL4* by YTH07-FLAG using RIP-qPCR. Our findings demonstrated that YTH07-FLAG pulled down more *OsCOL4* in *yth07* than in *ehd6 yth07* (Supplemental Figure 9A). This observation emphasized the importance of EHD6 for YTH07's efficient binding to *OsCOL4 in vivo*. Conversely, when an equal amount of the *EHD6-FLAG* construct was introduced into the protoplasts of *ehd6* and *ehd6 yth07*, no significant difference in the amount of *OsCOL4* pulled down by EHD6-FLAG was observed between *ehd6* and *ehd6 yth07* (Supplemental Figure 9B). These results suggested that the function of EHD6 is less dependent on YTH07, and again we attribute this to the redundancy within the YTH family in rice (Supplemental Figure 6A–6F).

Sequestration of *OsCOL4* mRNA in RNP granules represses the accumulation of OsCOL4 protein

It was reported that m^{6}A affects multiple aspects of mRNA metabolism, and YTH domain-containing m^{6}A readers have been shown to have multiple physiological roles, such as regulation of mRNA stability, splicing, alternative polyadenylation, and translation (Wei et al., 2018; Song et al., 2021; Chen et al., 2022; Wu et al., 2024). Given EHD6's collaborative role with YTH07 in efficient m^{6}A binding, we questioned whether EHD6 influences the metabolism of targeted mRNAs. qRT–PCR analysis revealed no apparent alteration in the mRNA abundance of *OsCOL4* in the *ehd6* mutant (Figure 6E). Furthermore, qRT–PCR analysis of RNP granules isolated from Dongjin and *ehd6* illustrated that more *OsCOL4* mRNAs were present in the RNP granules of Dongjin compared with those of

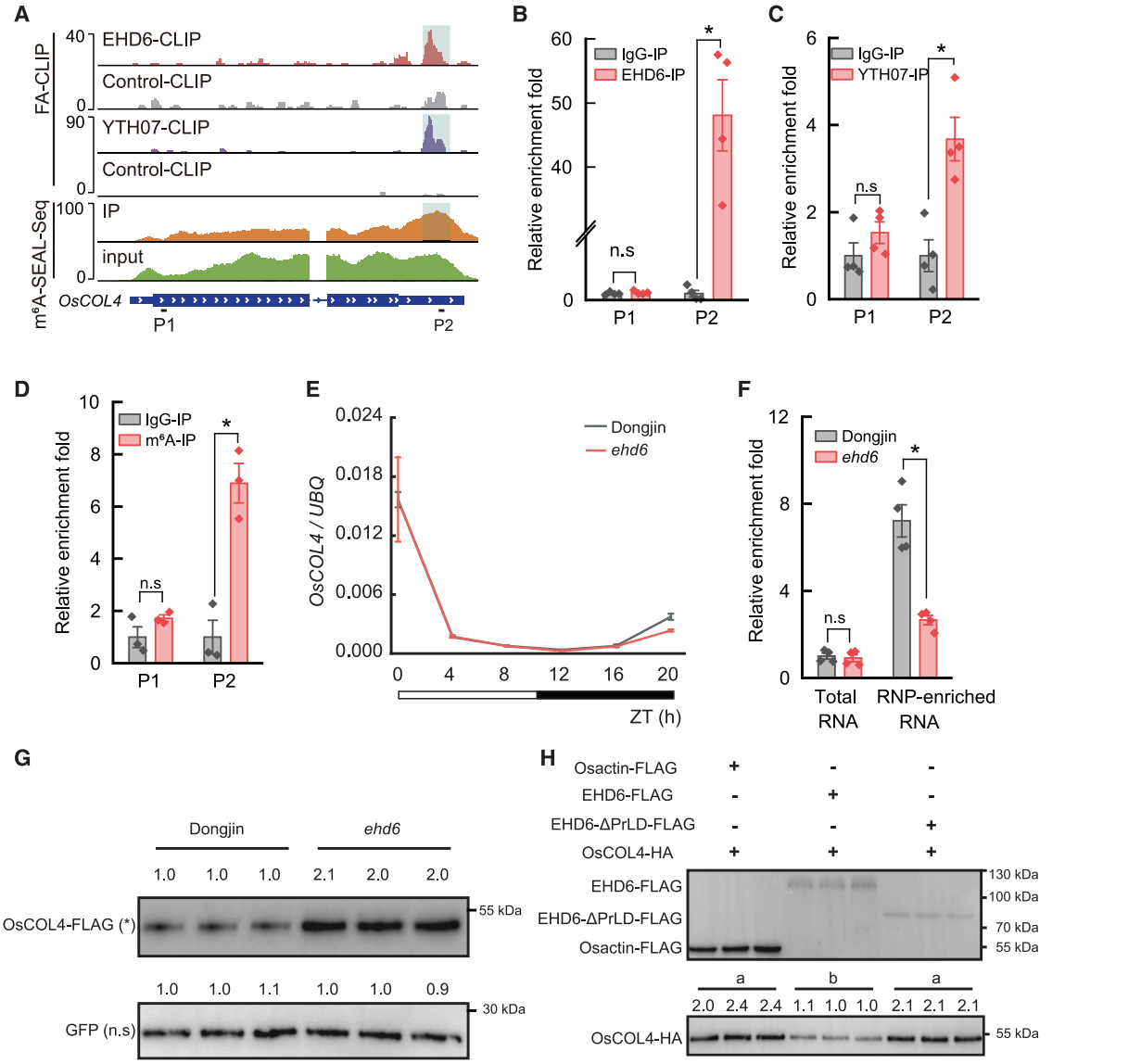

Figure 6. EHD6 sequesters *OsCOL4* mRNA in RNPs and affects OsCOL4 protein abundance.

(A) Integrative genomics viewer showing the indicated sequencing results for *OsCOL4*. Fragments (P1 and P2) amplified in **(B)–(D)** are labeled. The light blue box labeled in each sequencing result indicates the position of the m^{6}A site and the binding sites of EHD6 and YTH07.

(B) FA-RIP-qPCR verification of the ability of EHD6 to bind to *OsCOL4* in 3-week-old *pEHD6:EHD6-FLAG/ehd6* seedlings. Values are means ± SD; $n = 4$.

(C) FA-RIP-qPCR verification of the binding affinity of YTH07 for *OsCOL4* in 3-week-old *pYTH07:YTH07-GFP* seedlings. Values are means ± SD; $n = 4$.

(D) m^{6}A -IP-qPCR validation of the m^{6}A peak in *OsCOL4*. Values are means ± SD; $n = 3$.

(E) Rhythmic expression patterns of *OsCOL4* in Dongjin and the *ehd6* mutant under SD conditions. White and black boxes denote periods of light and darkness, respectively. Values are means ± SD; $n = 3$.

(F) qRT–PCR analysis of *OsCOL4* expression in the indicated RNAs from Dongjin and the *ehd6* mutant. Values are means ± SD; $n = 4$. In **(B)–(F)**, the rice *UBIQUITIN* gene was used as the internal control. * denotes significant difference determined by Student's *t*-tests ($P < 0.05$).

(G) Western blot analysis revealed a higher level of OsCOL4-FLAG protein accumulation in the protoplasts of *ehd6* compared with those of Dongjin. Proteins were detected with anti-FLAG and anti-GFP antibodies. GFP was employed as a non-EHD6 target control and showed no difference in protein accumulation across backgrounds. Three lanes in each group represent three biological repeats. * denotes significant difference and ns denotes no significant difference determined by Student's *t*-tests ($P < 0.05$).

(H) Western blot analysis shows a significantly higher protein abundance of OsCOL4-HA when it is co-expressed with EHD6-ΔPrLD in *ehd6* mutant protoplasts than when it is co-expressed with full-length EHD6. Osactin was used as a negative control; three lanes in each group represent three biological repeats. Different letters denote significant difference determined by one-way analysis of variance ($P < 0.05$).

the *ehd6* mutant (Figure 6F), which indicated that EHD6 condenses *OsCOL4* mRNAs into RNP granules. Considering that EHD6 co-localized with AtPAB2 (a canonical SG marker) (Supplemental Figure 7D and 7E), we speculated that EHD6 is able to arrest translation like SGs (Ripin et al., 2023; Wu et al., 2024). This led us to investigate the protein abundance of OsCOL4. We introduced a reporter with GFP driven by the 35S promoter (*35S:GFP*, a non-EHD6 target control) and an

OsCOL4-FLAG fusion protein driven by the maize ubiquitin promoter (*UBI:OsCOL4-FLAG*) into protoplasts of Dongjin and *ehd6*. Notably, the content of OsCOL4-FLAG protein in *ehd6* protoplasts was significantly higher than that in Dongjin protoplasts, while GFP protein abundance was equal in both backgrounds (Figure 6G). This indicated that EHD6 has a negative impact on the accumulation of OsCOL4 protein.

To further confirm this finding, we generated transgenic plants stably expressing *OsCOL4-FLAG* in Dongjin and the *ehd6* mutant. The *FLAG* tag was used to distinguish endogenous and transgenic mRNAs. Five pairs of transgenic lines with comparable transcriptional levels of *OsCOL4-FLAG* in Dongjin and *ehd6* were selected for western blot analysis (Supplemental Figure 10A, 10C, 10E, 10G, and 10I). Upon quantifying the transcript and protein accumulation data from these five groups, we found that the protein abundance of OsCOL4-FLAG was significantly higher in the *ehd6* mutant background than in Dongjin (Supplemental Figure 10L) despite there being no significant difference in the expression of *OsCOL4-FLAG* between the Dongjin and *ehd6* backgrounds (Supplemental Figure 10K). Accordingly, the overexpression of *OsCOL4* with equal transcription levels resulted in a more pronounced delay in heading date in the *ehd6* mutant compared with the Dongjin background (Supplemental Figure 10A, 10M, and 10N). Similarly, when *OsCOL4* was overexpressed with lower transcription levels in the *ehd6* background compared with Dongjin, a similar delay in heading date was observed (Supplemental Figure 10C, 10O, and 10P). These findings strongly indicated that EHD6 promotes flowering by negatively impacting the accumulation of the OsCOL4 protein rather than modulating its transcription.

Next, we explored whether EHD6's condensation is crucial for inhibiting the accumulation of OsCOL4. We co-expressed either full-length EHD6 or EHD6-ΔPrLD (lacking condensation capability) with OsCOL4-HA in protoplasts derived from *ehd6*. Significantly, a higher protein abundance of OsCOL4-HA was observed when it was co-expressed with EHD6-ΔPrLD than when it was co-expressed with full-length EHD6 (Figure 6H), even though the transcription levels of *OsCOL4-HA* were equal (Supplemental Figure 11A). These findings suggested that EHD6 functions in preventing the accumulation of OsCOL4 protein and that this regulatory role is dependent on the PrLD domain-mediated phase separation.

To investigate whether YTH07 also influences the protein abundance of OsCOL4, since no difference in *OsCOL4* expression was observed between the *yth07* mutant and Dongjin (Supplemental Figure 12A), we employed the same reporter constructs used above: *35S*:*GFP* as a non-YTH07 target control and *UBI*:*OsCOL4-FLAG* for detecting the OsCOL4 protein levels. After introducing an equal amount of reporter construct into the protoplasts of Dongjin and *yth07*, we observed a higher abundance of OsCOL4-FLAG protein in *yth07* compared with Dongjin, while the abundance of GFP protein remained equal in both backgrounds (Supplemental Figure 12B). These results suggested that YTH07 inhibits the accumulation of OsCOL4 protein. Consistent with this, *Ehd1* (Lee et al., 2010), which acts downstream of OsCOL4, exhibited a significant reduction of expression in *yth07* (Supplemental Figure 12C).

Together, these results suggest that both EHD6 and YTH07 repress the accumulation of OsCOL4 protein, rather than altering its transcription level.

EHD6 promotes rice flowering through the *Ehd1* pathway

Previous studies reported that *OsCOL4* can repress flowering independently of photoperiod by negatively regulating the expression of *Ehd1* (Lee et al., 2010). Since EHD6 inhibits the accumulation of OsCOL4 protein, we further examined the expression of *Ehd1* and other key genes in the *ehd6* mutant and Dongjin. As expected, the mRNA abundances of *Ehd1* and the downstream florigen genes *Hd3a* and *RFT1* were lower in the *ehd6* mutant under LD and SD conditions (Figure 7A and Supplemental Figure 13A and 13B). However, other key flowering genes, including *DTH8*, *Ehd2*, *Ehd4*, *Ghd7*, *Hd1*, and *Hd2*, were similarly expressed in the *ehd6* mutant and Dongjin (Supplemental Figure 13C–13H). These observations suggested that *EHD6* regulates flowering through the *Ehd1* pathway. For verification, we created the *ehd1* mutant in the Nipponbare background using CRISPR-Cas9 (Supplemental Figure 13I), and the *ehd6-cr2 ehd1* double mutant was generated by crossing. The *ehd6-cr2 ehd1* double mutant showed a heading date very close to that of the *ehd1* single mutant under both NLD and NSD conditions, indicating that *Ehd1* is epistatic to *EHD6* (Figure 7B and 7C). Our results thus suggested that *EHD6* regulates flowering in rice through the *Ehd1* pathway.

DISCUSSION

m^{6}A is the most abundant modifier of mRNAs in higher eukaryotes. Accumulating evidence suggests that m^{6}A regulates various aspects of cellular physiology in both animals and plants (Roundtree et al., 2017; Shao et al., 2021). Readers are needed to implement the biological functions of m^{6}A methylation. Although YTH family m^{6}A readers have been identified both in mammals and plants, whether there is a need for an assistant component for efficient m^{6}A binding and how they act remain unexplored. In this study, we obtained several lines of evidence showing that the RBP EHD6 recruits the m^{6}A reader YTH07 for efficient m^{6}A binding and represses the accumulation of protein encoded by their target (*OsCOL4*) through phase separation to regulate flowering in rice.

Firstly, a conjoint analysis of EHD6-CLIP, YTH07-CLIP, and m^{6}A-SEAL-seq suggested that ∼80% (5796 out of 7263) of EHD6's targets were m^{6}A modified, and ∼80% (1397 out of 1751) of YTH07's target genes overlapped with those of EHD6 (Figure 4D). In addition, the binding sites of both EHD6 and YTH07 were enriched in the same region near the m^{6}A modification site of all their common targets (Figure 4E), and the enriched motifs of EHD6 and YTH07 resembled the canonical m^{6}A motif in plants (Supplemental Figure 5D). This evidence strongly indicates that EHD6 and YTH07 are highly associated with m^{6}A. Moreover, the interaction between EHD6 and YTH07 (Figure 2E–2I), coupled with the stronger m^{6}A affinity of EHD6-YTH07 compared with EHD6 or YTH07 alone (Figure 4G), suggested that EHD6 can cooperate with YTH07 to efficiently bind m^{6}A.

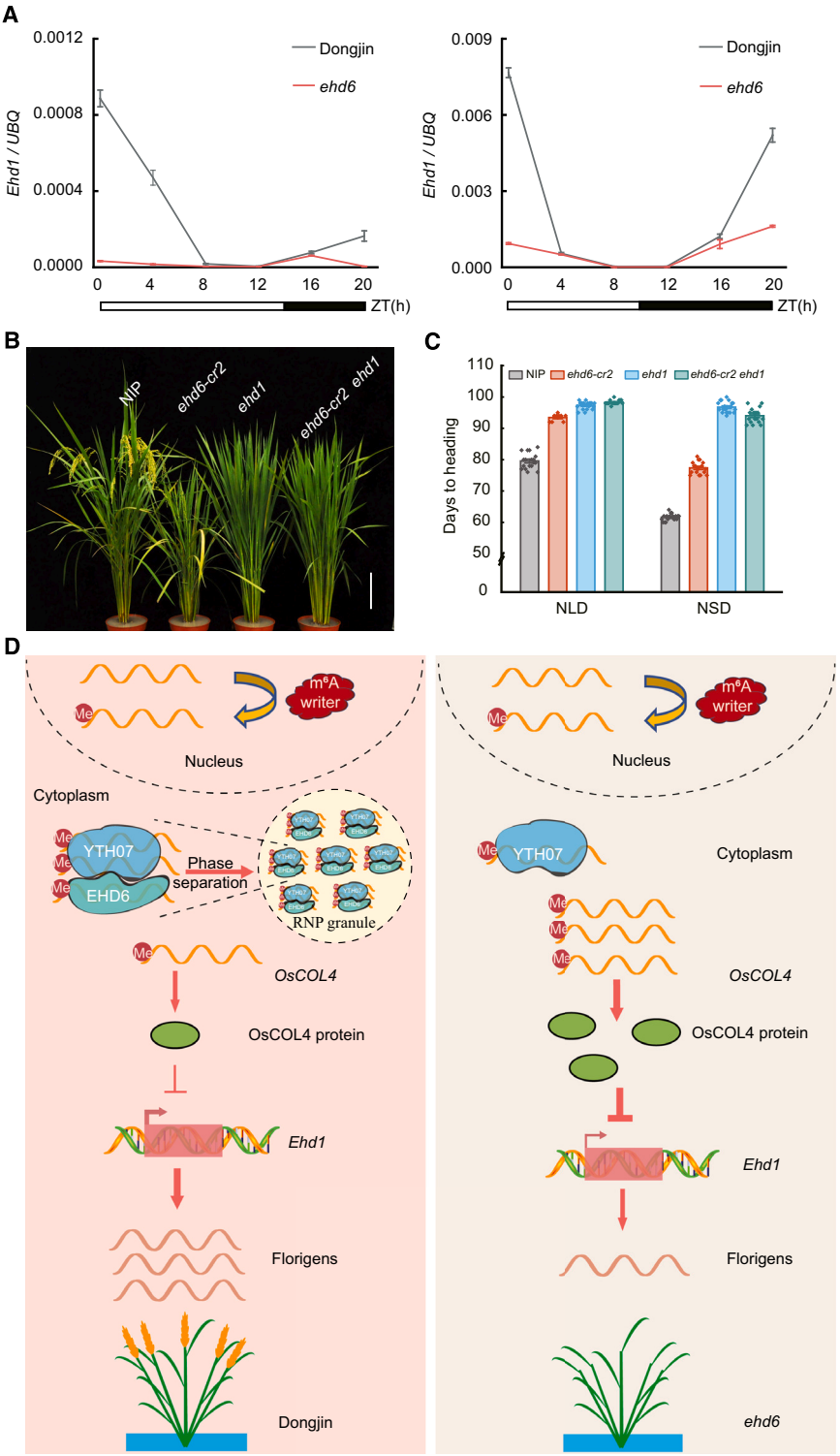

Figure 7. EHD6 promotes flowering through the *Ehd1* pathway.

(A) qRT–PCR analysis of rhythmic expression of *Ehd1* in Dongjin and the *ehd6* mutant under LD (left) and SD (right) conditions. The rice *UBIQUITIN* gene was used as the internal control. Values are means ± SD; $n = 3$. White and black boxes denote light and dark periods, respectively.

(B and C) Phenotypes and heading dates of Nipponbare (NIP), *ehd6-cr2*, *ehd1*, and the *ehd6-cr2 ehd1* double mutant under NLD conditions. The *ehd6-cr2*, *ehd1*, and *ehd6-cr2 ehd1* mutants are all in the NIP background. Scale bar corresponds to 20 cm. Values are means ± SD; $n > 9$.

(D) A model depicting the function of EHD6 in flowering control. Transcripts of *OsCOL4* are methylated by m^{6}A writers in the nucleus and transported to the cytoplasm. EHD6 not only binds the m^{6}A-modified mRNAs by itself, but also interacts with the m^{6}A reader YTH07, which boosts the affinity of EHD6 for the m^{6}A-modified *CONSTANS-like* mRNA (*OsCOL4*). The RNP comprising EHD6, YTH07, and m^{6}A-modified *OsCOL4* mRNA undergoes phase separation and moves to RNP granules where it inhibits the translation of *OsCOL4* mRNA. *OsCOL4* is a strong flowering repressor; reduction of its abundance releases repression of *Ehd1* and downstream florigen genes, resulting in early flowering. In the *ehd6* mutant, YTH07 has weaker m^{6}A binding ability and diffuses throughout the cytoplasm, leading to more free *OsCOL4* mRNAs and more OsCOL4 protein accumulation. In turn, the accumulation of OsCOL4 protein represses expression of *Ehd1* and downstream florigen genes, resulting in late flowering.

The observation that EHD6 can bind both m^{6}A and A, while YTH07 specially binds m^{6}A (Figure 4A and 4B), suggests that only YTH07 can distinguish m^{6}A and A *in vitro*. In addition, considering that YTH07 exhibits a superior capacity for m^{6}A binding compared with EHD6 (Figure 4A, 4B, and 4G), we propose that YTH07 primarily drives m^{6}A binding, while EHD6 plays a supportive role in facilitating YTH07's interaction with m^{6}A. Nevertheless, since both YTH07 and EHD6 have the ability to bind to m^{6}A (Figure 4A and 4B), the scenario where EHD6 and YTH07 bind to m^{6}A concurrently still cannot be dismissed.

It is widely recognized that m^{6}A readers fall into three categories (Shi et al., 2019). The first comprises the YTH family proteins, which possess a YTH domain enabling them to bind directly to m^{6}A. The second category is the heterogeneous nuclear ribonucleoproteins, often referred to as m^{6}A-switch. The third category includes RBPs such as FMR1 and IGF2BPs, which exhibit a preference for binding to m^{6}A. EHD6, identified as an RBP with three RNA recognition motifs (Supplemental Figure 7B), has the ability to bind both m^{6}A and A (Figure 4A) and has an *in vivo* binding site enriched with m^{6}A (Figure 4C). These patterns closely align with the characteristics of the third category of m^{6}A readers. However, the relatively lower *in vitro* m^{6}A affinity of EHD6 (Figure 4A) compared with FMR1 and IGF2BPs in animals makes us hesitant to strictly define EHD6 as an m^{6}A reader. We lean toward defining EHD6 as a chaperone protein that assists YTH07 in

binding m^{6}A and plays a pivotal auxiliary role in m^{6}A recognition.

Secondly, we demonstrated that EHD6 colocalizes with SGs (Figure 5A and Supplemental Figure 7C–7E). YTH family m^{6}A readers were identified in a proteomic analysis of mammalian SG cores, suggesting that these non-membrane structures are closely associated with m^{6}A (Jain et al., 2016; Fu et al., 2020). It is worth noting that a previous study reported that EHD6 is localized in the nuclei of rice cells (Lyu et al., 2020). However, in this study, we observed no nuclear localization of EHD6 in *pEHD6:EHD6-GFP/ehd6* stable transgenic plants or in the rice protoplast and *N. benthamiana* leaf epidermal cell transient expression systems (Figure 5A and Supplemental Figure 7D and 7E). In addition, subcellular immunoblot analysis of the *pEHD6:EHD6-FLAG/ehd6* transgenic complementation lines revealed that the EHD6 protein was present exclusively in the cytoplasm (Supplemental Figure 7A). The discrepancy in the subcellular localization of EHD6 may be due to the difference in genetic backgrounds. As EHD6 was reported to be phosphorylated by GLYCOGEN SYNTHASE KINASE 2 (Lyu et al., 2020), it would be intriguing to investigate whether the phosphorylation state of EHD6 affects its subcellular localization.

Thirdly, despite the well-known roles of m^{6}A modification in regulating mRNA stability and promoting translation, genome-level evidence suggests that m^{6}A can also be involved in translation repression (Ries et al., 2019; Liu et al., 2023). Similarly, *cis*-m^{6}A QTL mapping in human cells found that quite a lot of m^{6}A-targeted mRNAs have reduced translation efficiency, raising the possibility that specific RBPs mediate translation repression (Zhang et al., 2020). However, there is limited direct biochemical and genetic evidence to substantiate this notion. In this study, we found that, with equal transcription levels (Supplemental Figure 10K), the protein level of OsCOL4-FLAG was higher in the *ehd6* mutant than in wild-type background transgenic plants (Supplemental Figure 10L), suggesting that EHD6 plays a negative role in the accumulation of its target protein. Considering that EHD6 is an RBP and interacts with the m^{6}A reader YTH07, the EHD6-YTH07 interaction could be an example of translation repression mediated by the interaction between an RBP and an m^{6}A reader in plants.

Moreover, we discovered that EHD6 can trigger the relocation of YTH07 to RNP granules through a phase separation mechanism (Figure 5D–5H). This observation aligns with previous reports that m^{6}A-containing mRNAs can enhance the phase separation potential of YTHDF proteins and promote SGs formation (Ries et al., 2019; Fu et al., 2020). SGs were initially described in mammalian cells subjected to heat shock and later found to be associated with human chronic diseases such as amyotrophic lateral sclerosis, frontotemporal degeneration, and Alzheimer's disease (Riggs et al., 2020). SG protein aggregation is also linked to animal aging and lifespan (Lechler et al., 2017; Cao et al., 2020), suggesting that SGs can also form stably independently of short-term stress stimulation. Interestingly, we observed that EHD6 formed foci in the cytosol and co-localized with the SG marker AtPAB2 under normal conditions (Figure 5A and Supplemental Figure 7D and 7E), which is distinct from the stress-induced SG-localized m^{6}A readers, such as *Arabidopsis* ECT2 (Scutenaire et al., 2018). Strikingly, the SG marker AtPAB2 exhibited focal localization pattern in the presence of EHD6 even at normal temperatures (Supplemental Figure 7D–7F). This suggested that EHD6 can condense other proteins, including AtPAB2. This led us to suspect that what EHD6 localizes to is not a typical SG, although EHD6 co-localized with the SG marker AtPAB2 under both normal and stress conditions. Therefore, we use the term "RNP granules," which encompass various membraneless granule structures in the cytoplasm, to describe the localization of EHD6. Considering that SG formation provides an elegant mechanism to arrest mRNA translation in response to stress (Kosmacz et al., 2019; Ripin et al., 2023), we hypothesize that the condensation of EHD6 and YTH07 sequesters the *OsCOL4* mRNA from the translation machinery, or exhibits reduced dynamics, consequently attenuating translation and ultimately leading to a decrease in the OsCOL4 protein level.

In addition, it is worth pointing out that the *ehd6* mutant shows a more pronounced late flowering phenotype than the *yth07* knockout lines (Figures 1A, 1B, 3A, and 3B). A comparative analysis of the interdependence between EHD6 and YTH07 in m^{6}A and *OsCOL4* binding reveals that the absence of EHD6 weakens YTH07's capacity to bind m^{6}A and *OsCOL4* (Figure 4I and Supplemental Figure 9A). However, the absence of YTH07 does not significantly alter EHD6's ability to bind m^{6}A and *OsCOL4* (Supplemental Figures 5F and 9B). One possible explanation for this observation could be redundancy among the 12 members of YTH family in rice (Supplemental Figure 6A). Further knockout of YTH family members using CRISPR-Cas9 could identify more regulators involved in the EHD6-mediated m^{6}A-dependent flowering pathway.

In summary, we discovered EHD6, an RBP that can interact with the m^{6}A reader YTH07. EHD6-YTH07 can efficiently bind m^{6}A-modified *OsCOL4* mRNA, triggering phase separation and the formation of RNP granules. Consequently, this process prevents translation of *OsCOL4* in the cytoplasm, thereby reducing the protein abundance of OsCOL4. As a result, the expression of the key floral integrator gene *Ehd1* is promoted, leading to an acceleration of flowering under both LD and SD conditions (Figure 7D). Our results elucidate a mechanism whereby EHD6 collaborates with YTH family proteins for efficient m^{6}A recognition and condenses m^{6}A-modified mRNAs to form RNP granules. This discovery reveals a potential role of m^{6}A in translation repression, providing significant insight into the post-transcriptional regulation of rice flowering. Since *EHD6* promotes flowering under various conditions, this finding provides a mechanism to adjust heading date without altering the photoperiod or temperature response. Thus, both *EHD6* and *YTH07* could serve as targets for rice breeders to optimize flowering in different geographical regions.

METHODS

Plant materials and growth conditions

The *ehd6* mutant was obtained from the progeny of a transgenic line in the Dongjin (*O. sativa* L. ssp. *japonica*) background, but it has no T-DNA insertion, so the mutation likely comes from tissue culture-mediated mutagenesis. All plants for phenotypic observation were grown in Nanjing (31°14′N, 118°22′E) during the

summer, representing NLD conditions, and at Lingshui (18°22′N, 109°45′E) during the winter, representing NSD conditions. Plants were also grown in climate chambers under CLD (14 h light/10 h darkness, 28°C) and CSD (10 h light/14 h darkness, 28°C) conditions to observe the phenotype and examine the expression of flowering-related genes. To determine whether the heading date difference between Dongjin and the *ehd6* mutant was affected by the environment, we planted the materials at Beijing (39°90′N, 116°30′E), Lianyungang (35°07′N, 119°48′E), Xuzhou (34°15′N, 117°11′E), Huaian (33°36′N, 119°01′E), Nanchang (29°11′N, 116°35′E), and two locations at similar latitudes (22°48′N, 103°13′E and 22°39′N, 101°4′E) in Yunnan Province that differed by more than 1200 m in altitude, creating a more than 7°C temperature difference under similar photoperiod conditions.

Identification of *EHD6* by bulked segregant analysis

The *ehd6* mutant was crossed with Dongjin to produce an F_2 population; leaf tissues from 30 early-flowering and 30 late-flowering F_2 plants were separately pooled. Genomic DNAs of the two pools were extracted using the CTAB method followed by isopropanol precipitation and sequenced using next-generation sequencing (Illumina, coverage: ∼30×). A modified MutMap pipeline (Fekih et al., 2013) was used to identify the causal mutation. The candidate mutation site was confirmed in more individual F_2 plants by Sanger sequencing.

Vector construction and plant transformation

The full-length CDS of *EHD6* driven by its native promoter (2.0 kb) was cloned into the binary vector pCAMBIA1390-FLAG (or pCAMBIA-1305.1) to generate the *pEHD6*:*EHD6-FLAG* (or *pEHD6:EHD6-GFP*) construct for complementation tests. *Agrobacterium tumefaciens* strain EHA105 cells containing the resultant plasmid were introduced into calli of the *ehd6* mutant. Expression of the target gene in T_0 transgenic lines was verified using western blot analysis, and positive T_1 transgenic lines were phenotyped for heading date.

To develop the *ehd6*, *ehd1*, and *yth07* single mutants, we knocked out the genes using genomic editing vectors containing 20-bp gene-specific spacer sequences targeting *EHD6*, *Ehd1*, or *YTH07* in the pYLCRISPR-Cas9P$_{ubi}$-H backbone (Ma et al., 2015). The resultant plasmids were transformed into *A. tumefaciens* strain EHA105 and then separately introduced into calli of Nipponbare and Dongjin. The edited T_0 transgenic lines were analyzed by Sanger sequencing, and homozygous T_1 lines were selected for phenotyping.

Primers used in vector construction and transgenic plant identification are listed in Supplemental Table 4.

Gene expression analysis

Leaf samples from Dongjin and *ehd6* mutant plants grown under CLD (50 days after sowing) or CSD (27 days after sowing) conditions were collected to investigate diurnal expression of flowering-related genes. Total RNA was isolated from frozen tissues using an RNAprep Pure Plant kit (TIANGEN, DP432) according to manufacturer's manual, and total RNA was extracted from protoplasts using the Trizol (Invitrogen, 15596018CN) method followed by isopropanol precipitation. Total RNA was reverse transcribed using PrimeScript II Reverse Transcriptase (Takara, 2690A) with Oligo(dT) 18 primer. qRT–PCR was performed with TB Green Premix Ex Taq (Takara, RR420A) according to the operation manual. Rice *Ubiquitin* (*UBQ*) was used as the internal control.

A 3.2-kb promoter was cloned into pCAMBIA-1305.1 to create the *pEHD6:GUS* construct, and the resultant plasmid was transformed into Dongjin. Primers used for vector construction are listed in Supplemental Table 4. Fresh samples from the *pEHD6:GUS* transgenic plants were incubated for 4 h in a staining buffer (50 mM $NaH_2PO_4·2H_2O$, 50 mM $Na_2HPO_4·2H_2O$, 1 mM $K_3[Fe(CN)_6]$, 1 mM $K_4[Fe(CN)_6]$, 10 mM EDTA, 0.1% Triton X-100, 1 mg/ml X-GluC) in darkness at 37°C. The stained tissues were cleared with 70% ethanol for imaging.

Subcellular localization

Transient expression assays were performed on rice leaf protoplasts and *N. benthamiana* leaves. The full-length CDSs of *EHD6* and *YTH07* were amplified and separately cloned into the pCAMBIA-1305.1 vector to produce the *p35S:EHD6-GFP* and *p35S:YTH07-GFP* constructs. The method for rice leaf protoplast preparation and transformation was described in a previous study (Zhang et al., 2011). The subcellular localization of the EHD6 and YTH07 proteins was also observed in *N. benthamiana* leaves. GFP was fused to the C termini of EHD6 and YTH07, as well as three different truncated domain forms of EHD6, under the control of the 35S promoter in the vector pCAMBIA-1305.1; mCherry was also fused to the C terminus of YTH07 when it was co-expressed with EHD6-GFP. The EHD6-GFP fusion, ECT2-GFP fusion, SG marker (AtPAB2-mCherry), P-body marker (AtDCP1-mCherry), YTH07-GFP fusion, YTH07-mCherry fusion, EHD6-ΔN-RRM-GFP, EHD6-ΔPrLD-GFP, and EHD6-ΔC-RRM-GFP constructs were transformed into the *A. tumefaciens* strain EHA105. Activated cells were harvested, resuspended in induction medium (10 mM $MgCl_2$, 10 mM MES-KOH [pH 5.7], 200 μM AS), and incubated at 28°C for 2–4 h. Then the mixed *A. tumefaciens* strains were infiltrated into 4- to 5-week-old *N. benthamiana* leaves. Fluorescence signals were detected using a Leica TCS SP8 confocal microscope 48 h after infiltration. Primers used in the assay are listed in Supplemental Table 4.

For subcellular immunoblot analysis, the subcellular fractions were isolated using a Minnte Plasma Membrane Protein Isolation for Plant (Invent Biotechnologies, SM-005-P) according to the manufacturer's manual. For immunoblotting, Anti-FLAG (Sigma, A8592), Anti-HSP (Beijing Protein innovation, AbM51099-31-PU), and Anti-H3 (Abcam, ab1791) were used.

To observe the protein subcellular location in transgenic rice, GFP was fused to the C termini of EHD6 and YTH07 under the control of their native promoters. The *pEHD6:EHD6-GFP* construct was introduced into the *ehd6* background, and a transgenic complementation line was selected to observe the GFP fluorescence in roots. Meanwhile, the *pYTH07:YTH07-GFP* construct was introduced into the COM13 (EHD6-FLAG complementation line) background, and the GFP fluorescence in the

roots of transgenic lines was observed. 4′,6-diamidino-2-phenylindole (1 μg/ml) was used to mark cell nuclei.

Yeast two-hybrid assay

Yeast two-hybrid screening was performed following the Matchmaker GAL4 Two-Hybrid System manual (Clontech). The full-length CDS of *EHD6* was amplified and cloned into the pGBKT7 vector, and then transformed into the yeast strain AH109. The EHD6 protein was used as a bait to screen a cDNA library (in the Y187 strain) prepared from equal amounts of mRNAs from 50-day-old (CLD conditions) and 27-day-old (CSD conditions) mixed rice leaves (ZT0, ZT4, ZT8, ZT12, ZT16, and ZT20). For confirmation of interaction, the CDS of *YTH07* was inserted into the pGADT7 vector and various plasmid combinations were co-transformed into yeast strain AH109 according to manufacturer's manual. Combinations of the respective empty pGADT7 or pGBKT7 vectors were used as negative controls. Yeast strains with the combinations were spread onto SD/-Trp/-Leu plates and incubated at 30°C for 3–5 days. Clones were then plated onto SD/-Ade/-His/-Leu/-Trp dropout screening medium to test for protein interaction. Primers are listed in Supplemental Table 4.

BiFC analysis

The CDSs of *EHD6*, *YTH07*, other YTH family members, and truncated variants of *YTH07* were separately inserted into the P_2YN and P_2YC vectors and introduced into *A. tumefaciens* strain EHA105. Combinations with empty P_2YN or P_2YC were used as negative controls. Activated cells were harvested, resuspended in induction medium, and incubated at 28°C for 2–4 h. The mixed *A. tumefaciens* strains were infiltrated into 4- to 5-week-old *N. benthamiana* leaves. Fluorescence signals were detected using a Leica TCS SP8 confocal microscope 48 h after infiltration. Primers are listed in Supplemental Table 4.

Pull-down assay

To detect the interaction between EHD6 and YTH07, other YTH family members, and truncated variants of YTH07 *in vitro*, the CDS of *EHD6* was amplified and cloned into the vector pMAL-c2X, and the CDSs of *YTH07*, other YTH family members, and truncated variants of *YTH07* were amplified and cloned into the vector pGEX-4T-2. Then the MBP-EHD6, GST-YTHs, GST-N-YTH07/M-YTH07/C-YTH07, and GST proteins were expressed in cells of *Escherichia coli* strain BL21 (DE3) under induction with 0.5 mM isopropyl β-D-thiogalactopyranoside (IPTG) while shaking at 16°C for 22 h. The *E. coli* cells were collected and resuspended in PBS buffer (137 mM NaCl, 2.7 mM KCl, 10 mM Na_2HPO_4, 2 mM KH_2PO_4). The resuspended liquid was sonicated to break the cells until the liquid was clear (cycles of 3 s on, 10 s off) and then centrifuged at 15 000 *g* for 10 min to collect the supernatant for pull-down analysis. Roughly equal amounts of GST or GST-YTH07/N-YTH07/M-YTH07/C-YTH07 protein were mixed with GST MA (Solarbio, M2320) at 4°C for 1 h, and then incubated with MBP-EHD6 at 4°C for an additional 1 h before the next incubation, taking a small amount as input. The agarose was washed six times with PBS (with an additional 0.5% IGEPAL CA-630 [Sigma, I8896] and 400 mM NaCl) and then boiled with protein loading buffer (50 mM Tris–HCL [pH 6.8], 2% SDS, 10% glycerol, 0.1% bromophenol blue, and 1% β-mercaptoethanol) at 100°C for 5 min. The proteins were separated in 4%–20% SDS–PAGE gels (GenScript, M00656) and detected by western blot analysis using anti-GST antibodies (Abmart, M20007L) and anti-MBP antibodies (NEB, E8032L).

Co-immunoprecipitation (Co-IP) assay

To detect interaction between EHD6 and YTH07 *in vivo*, the CDS of *EHD6* was amplified and cloned into the pCAMBIA1390-FLAG vector to produce the EHD6-FLAG construct, and the CDS of *YTH07* was inserted into pCAMBIA-1305.1 to produce the YTH07-GFP construct. Both constructs were introduced into *A. tumefaciens* strain EHA105. Activated cells were harvested, resuspended in the above induction medium, and incubated at 28°C for 2–4 h. The mixed *A. tumefaciens* combinations were infiltrated into 4- to 5-week-old *N. benthamiana* leaves, and after 72 h 3 g of leaf tissue with veins removed was ground into a fine powder in liquid nitrogen. Immediately after turning dark green, the sample was resuspended in NB1 buffer (50 mM Tris–MES [pH 8.0], 10 mM EDTA, 0.5 M sucrose, 1 mM $MgCl_2$, 5 mM DTT and 1× protease inhibitor cocktail [Roche, 11836170001]). The samples were thoroughly mixed, incubated with rotation at 4°C for 30 min, and centrifuged at 15 000 rpm for 20 min at 4°C. Protein G MA (Millipore, LSKMAGG10) was washed twice with NB1 buffer, added to the sample lysate, and incubated at 4°C for 1 h for prehybridization. A portion of the supernatant was saved as the input, and the remaining portion was incubated with pre-cleaned GFP Magnetic Agarose beads (MBL, D153-10) at 4°C for 2 h. Subsequently, the agarose beads were washed thrice with NB1 buffer (including 0.1% IGEPAL CA-630) and then resuspended in NB1 buffer. To elute the bound protein from the agarose, the mixture was boiled with protein loading buffer (containing 50 mM Tris–HCL [pH 6.8], 2% SDS, 10% glycerol, 0.1% bromophenol blue, and 1% β-mercaptoethanol) for 5 min at 100°C. The immunoprecipitated proteins, along with the protein extracts from the input, were separated using 4%–20% SDS–PAGE gels and subsequently detected using Anti-FLAG antibodies (Sigma, A8592) and Anti-GFP antibodies (GenScript, A01388). Primers are listed in Supplemental Table 4.

To better illustrate the interaction of EHD6 and YTH07 *in vivo*, the CDSs of *YTH07* and *GFP* were separately cloned into the pAN580-HA vector to produce the YTH07-HA and GFP-HA constructs. These constructs were separately transformed into the protoplasts of EHD6-FLAG complementation lines. The method for rice leaf protoplast preparation and transformation was described in a previous study (Zhang et al., 2011). We performed Co-IP assays using HA Magnetic Agarose beads (MBL, M180-10), and the steps for this method are similar to those for the Co-IP method for *N. benthamiana* leaves.

FA-CLIP

FA-CLIP was conducted following the protocol described previously (Song et al., 2021). Three grams of 21-day-old rice leaves from plants (*ehd6*, *pEHD6:EHD6-FLAG/ehd6*, and transgenic seedlings expressing YTH07-GFP [*pYTH07:YTH07-GFP*] introduced into COM13 [*pEHD6:EHD6-FLAG*]) grown under CSD conditions for each biological replicate were fixed in 37 ml of 1% formaldehyde solution for 15 min at room temperature under vacuum, after which 2.5 ml of 2 M glycine solution was added to quench the reaction for 5 min under vacuum. The fixed samples were then

frozen in liquid nitrogen and ground thoroughly with a TissueLyser II (QIAGEN) at 30 Hz for 2 min. Subsequently, 3 ml of lysis buffer (150 mM KCl, 50 mM HEPES [pH 7.5], 2 mM EDTA, 1% NP-40, 0.5 mM DTT, 1× cocktail protease inhibitor, and 40 U/ml RNase inhibitor) was added. The mixture was incubated at 4°C with gentle rotation for 20 min. These lysates were centrifuged at 13 000 rpm for 15 min at 4°C, and the supernatants were filtered using a 0.22-μm membrane filter. Then, 3 μl of Turbo DNase (Thermo, AM2238) and 3000 U of RNase T1 (Thermo, EN0541) were added, followed by a 15-min incubation at 22°C. Meanwhile, 25 μl of Anti-FLAG M2 Magnetic beads (Sigma, M8823) and GFP-Trap magnetic beads (Chromotek, gtma) per sample were washed with low-salt wash buffer (300 mM KCl, 50 mM HEPES [pH 7.5], 0.05% NP-40, 0.5 mM DTT, and 1× protease inhibitor). The washed beads and the sample solution were incubated at 4°C for 3 h. The beads were collected, washed three times with low-salt wash buffer, and resuspended in 396 μl of low-salt wash buffer with 4 μl of RNase T1 added, followed by a 15-min incubation at 22°C. After three washes with high-salt wash buffer (500 mM KCl, 50 mM HEPES [pH 7.5], 0.05% NP-40, 0.5 mM DTT, and 1× protease inhibitor), the beads were proceeded to end repair and phosphorylation. Finally, the beads were digested with proteinase K, and the RNA was recovered with RNA Clean & Concentrator-5 (Zymo, R1014) followed by library construction using the NEBNext Small RNA Library Prep Set for Illumina.

RIP-qPCR

The FA-RIP-qPCR assay was performed following a previously described procedure (Song et al., 2021). In brief, leaves from 21-day-old transgenic plants expressing EHD6-FLAG and YTH07-GFP were separately fixed with 1% formaldehyde solution. The fixed plant materials were ground into powder and incubated with lysis buffer in head-over-tail rotation for 30 min at 4°C. After full lysis and centrifugation, the lysates were collected and digested with RNase T1, and then immunoprecipitated with pre-washed Anti-FLAG M2 beads, Anti-GFP beads, or a control IgG conjugated with protein A Dynabeads on a rotating wheel for 2 h at 4°C. After washing and proteinase K digestion, the RNA fractions were recovered and reverse transcribed into cDNA to calculate the relative enrichment fold via qRT–PCR. *UBQ* was used as the internal control.

When conducting RIP-qPCR using protoplasts, the procedure was largely identical to that when using leaf tissue, with the exception that there was no vacuum applied during the formaldehyde cross-linking process, and RNase T1 was not employed for digestion.

m^{6}A-IP-qPCR

We conducted m^{6}A-IP enrichment followed by qRT–PCR to quantify changes in the m^{6}A methylation level of a specific target m^{6}A site. In brief, 0.5 μg of fragmented poly(A)+ RNA extracted from 21-day-old Dongjing plants was supplemented with 1 μl of 1:100 diluted m^{6}A and non-m^{6}A spike-in from the EpiMark *N*^{6}-Methyladenosine Enrichment Kit (NEB, E1610S). Subsequently, m^{6}A-IP was performed using the EpiMark *N*^{6}-Methyladenosine Enrichment Kit following the manufacturer's protocols. RNA from both the IP and Input fractions was then extracted via acid phenol/chloroform extraction and subjected to qRT–PCR. The spike-in served as a reference gene during qPCR analysis.

Isolation of RNP granules

RNP granules were isolated as described previously (Kosmacz et al., 2019). Twenty-one-day-old leaves (Dongjin and *ehd6* mutant) were ground to a fine powder in liquid nitrogen and extracted in a lysis buffer (50 mM Tris–HCl [pH 7.4], 100 mM potassium acetate, 2 mM magnesium acetate, 0.5% NP-40, 0.5 mM DTT, 1 mM sodium fluoride, 1 mM sodium orthovanadate, 1× cocktail protease inhibitor, and 40 U/ml RNase inhibitor) at 4°C for 30 min. After centrifugation at 4000 *g* for 10 min, the supernatant was removed and the pellet containing RNPs was resuspended in the lysis buffer. After the suspension was centrifuged at 18 000 *g* for 10 min at 4°C, the pellet was resuspended in the lysis buffer. This step was repeated once. The suspension containing RNPs was collected after a final centrifugation at 850 *g* for 10 min at 4°C.

RNA EMSA

To perform the RNA EMSA, the CDSs of *EHD6*, *YTH07*, and YTH07-ΔYTH were inserted into the pGEX-4T-2 vector. The GST-EHD6, GST-YTH07, GST-YTH07-ΔYTH, and empty GST constructs were introduced into *E. coli* strain DE3, and protein production was induced by culturing cells in 0.5 mM IPTG at 16°C for 20 h. The induced proteins were sonicated, purified with GST MA (Solarbio, M2320), and eluted with 10 mM GSH (10 mM GSH, 50 mM Tris [pH 8.0]). EMSA was performed using a LightShift Chemiluminescent RNA EMSA Kit (Thermo Scientific, 20158), according to the manufacturer's protocol. The probes are listed in Supplemental Table 2.

In vitro phase separation

In vitro phase separation was conducted as reported previously (Wang et al., 2020a, 2023). Purified recombinant GFP-EHD6, YTH07, and GFP kept in stock solution (20 mM HEPES [pH 7.4], 150 mM KCl, 1 mM DTT) were used for the phase separation test. To check the influence of RNA on phase separation, GFP-EHD6 was mixed gently with CY5-m^{6}A or CY5-A (5 μM) in the presence or absence of YTH07. GFP was used as a control. After incubation at room temperature for 10 min, 5 μl of solution was transferred to glass slides and imaged by a TCS SP8 confocal laser scanning microscope (Leica). The probes are listed in Supplemental Table 2.

FRAP

FRAP of EHD6-GFP or YTH07-mCherry proteins located in cytoplasmic foci in tobacco was performed as described previously (Rosa, 2018). The TCS SP8 confocal laser scanning microscope (Leica) was used, and a region of the EHD6-GFP or the YTH07-mCherry foci was bleached using a 488- or 587-nm laser pulse on a 20× objective. Recovery was recorded for a total of 120 s after bleaching. All experiments were repeated three times for each measurement.

In vivo RIP followed by LC–MS/MS for m^{6}A quantification

RIP was performed using a procedure similar to that used for RIP-qPCR but without the RNase T1 digestion. The FA-fixed 21-day-old *pEHD6:EHD6-FLAG/ehd6* transgenic seedlings or protoplasts transiently expressing EHD6-FLAG and YTH07-GFP were divided into two equal parts: one part for

immunoprecipitation with FLAG M2 Magnetic beads (Sigma, M8823) or GFP MA (MBL, D153-10), and the other for immunoprecipitation with normal rabbit IgG (Sigma, I5006-50mg) bound to Protein G MA (Millipore, LSKMAGG10). After washing and ethanol precipitation, the m^{6}A level in the recovered RNA fractions was measured by LC–MS/MS.

The LC–MS/MS was performed as follows: RNA (200–300 ng) was digested with 1 unit of Nuclease P1 (Wako, 145-08221) in 40 μl buffer containing 10% 0.1 M ammonium acetate (pH 5.3) at 42°C for 4 h, followed by the addition of 1 unit of shrimp alkaline phosphatase (NEB, M0371S) and 10% Cutsmart buffer at 37°C for 3 h, and the aqueous phase was injected for LC–MS/MS. Nucleosides were separated by reversed-phase ultra-performance liquid chromatography on a Kinete 2.6 μm F5 100 Å column with on-line mass spectrometry detection using liquid chromatography coupled to triple quadrupole mass spectrometry (Triple Quad 6500+, AB Siex) in positive electrospray ionization mode. The nucleosides were quantified by using the nucleoside to base ion mass transitions of 282–150 (m^{6}A) and 268–136 (A). Quantification was performed in comparison with the standard curve obtained from pure nucleoside standards run with the same batch of samples. The ratio of m^{6}A to A was calculated based on the calibrated concentrations. All experiments were repeated three times.

Determination of protein abundance

To determine the mRNA and protein abundances of *OsCOL4* in Dongjin and the *ehd6* mutant, *OsCOL4* was amplified and cloned into the binary vector pCAMBIA1390-FLAG to generate the *pUBI*:*OsCOL4-FLAG* construct. The plasmid was then transformed into *A. tumefaciens* strain EHA105 and separately introduced into Dongjin and the *ehd6* mutant. Expression of the target genes in T_0 transgenic plants was analyzed using qRT–PCR, and primers were designed to specifically target the exogenous *OsCOL4-FLAG*. Lines with comparable *OsCOL4-FLAG* expression levels in the *ehd6* mutant and Dongjin were selected for comparison of the abundance of the OsCOL4-FLAG fusion protein. Positive T_1 transgenic lines were selected for phenotyping.

To detect protein abundance in rice protoplasts, we inserted GFP driven by the 35S promoter (*p35S*:*GFP*) into the recombinant *pUBI*:*OsCOL4-FLAG* construct. GFP was used as the non-EHD6 (or YTH07) target control. The method for rice leaf protoplast preparation and transformation was described in a previous study (Zhang et al., 2011).

To determine the importance of the PrLD domain for EHD6-mediated inhibition of OsCOL4 accumulation, we co-expressed full-length EHD6, EHD6-ΔPrLD (incapable of condensation), or Osactin (Os03g0718100, as a negative control) with the OsCOL4-HA construct in protoplasts derived from *ehd6*. Anti-FLAG was used to detect EHD6-FLAG, EHD6-ΔPrLD-FLAG, and Osactin-FLAG. Anti-HA was used to detect OsCOL4-HA.

Data analysis for m^{6}A-SEAL-seq

The m^{6}A-SEAL-seq data (GSE129979) were downloaded from NCBI GEO datasets. Adapter trimming and size selection were performed using Cutadapt (v4.4) to retain fragments with a length of 20 nt or greater. The sequences were then mapped to the reference genome (IRGSP-1.0) with HISAT2 (v2.2.1) (Kim et al., 2015) using default parameters. The m^{6}A-enriched regions were extracted using the MACS2 peak-calling algorithm (Dominissini et al., 2013) based on default enrichment (IP/Input) parameters and $P < 0.01$.

Data analysis for FA-CLIP

After adapter trimming with Cutadapt (v1.18), the reads ≥20 nt in length were filtered out and mapped to the reference genome (IRGSP-1.0) using HISAT2 (v2.1.0) (Kim et al., 2015) with default parameters. Peak calling was conducted based on default IP enrichment parameters (FA-CLIP-IP/FA-CLIP-CONTROL) and false discovery rate < 0.05 with the MACS algorithm (Dominissini et al., 2013) to identify significant EHD6 or YTH07 binding sites.

DATA AVAILABILITY

The raw EHD6 FA-CLIP and YTH07 FA-CLIP sequencing data reported in this paper have been deposited in the BIG Data Center (http://bigd.big.ac.cn) under project number PRJCA024711. The published m^{6}A-SEAL-seq data can be downloaded from the NCBI database (GSE129979).

SUPPLEMENTAL INFORMATION

Supplemental information is available at *Molecular Plant Online*.

FUNDING

This work was supported by the Key Laboratory of Biology, Genetics and Breeding of Japonica Rice in Mid-lower Yangtze River, Ministry of Agriculture and Rural Affairs, China, and the Jiangsu Collaborative Innovation Center for Modern Crop Production, China. Funding for this work was provided by the National Key Research and Development Program of China (2020YFE0202300 and 2021YFD1200504), the National Natural Science Foundation of China (31971910 and 32272115), and the National Science Foundation of Jiangsu Province (BK20212010 and BK20230038), and the Foundation of Biological Breeding Zhongshan Lab (BM2022008-03, ZSBBL-KY2023-04, and ZSBBL-KY2023-06).

AUTHOR CONTRIBUTIONS

S.C. and S.Z. designed the study. S.C. performed most of the experiments with the help of P.S.; C.W., S.C., B.H., Z.X., L.C., Y.H., L.Z., and H.H. performed part of the work. S.Z., H.D., Y.T., X.L., L.C., S.L., and L.J. provided technical assistance. X.C. and X.G. performed bioinformatic analysis. S.C., S.Z., H.W., and G.J. wrote the manuscript with comments from all authors. J.W. conceived the project and revised the manuscript.

ACKNOWLEDGMENTS

We thank Ms Shaoyan Lin and Yuanyuan Jia in the State Key Laboratory of Crop Genetics & Germplasm Enhancement and Utilization for the technical assistance in LC-MS/MSLC–MS/MS and protein interaction assays, Dr. Yehui Xiong in the Institute of Crop Science, Chinese Academy of Agricultural Sciences, for the guidance in RNA EMSA assays. No conflict of interest is declared. The authors declare no competing interests.

Received: October 22, 2023
Revised: March 31, 2024
Accepted: May 5, 2024
Published: May 7, 2024

REFERENCES

Arribas-Hernández, L., Bressendorff, S., Hansen, M.H., Poulsen, C., Erdmann, S., and Brodersen, P. (2018). An m^{6}A-YTH module

controls developmental timing and morphogenesis in *Arabidopsis*. Plant Cell **30**:952–967.

Arribas-Hernández, L., Simonini, S., Hansen, M.H., Paredes, E.B., Bressendorff, S., Dong, Y., Østergaard, L., and Brodersen, P. (2020). Recurrent requirement for the m^{6}A-ECT2/ECT3/ECT4 axis in the control of cell proliferation during plant organogenesis. Development **147**, dev189134.

Bian, X.F., Liu, X., Zhao, Z.G., Jiang, L., Gao, H., Zhang, Y.H., Zheng, M., Chen, L.M., Liu, S.J., Zhai, H.Q., and Wan, J.M. (2011). Heading date gene, *dth3* controlled late flowering in *O. Glaberrima* Steud. by down-regulating *Ehd1*. Plant Cell Rep. **30**:2243–2254.

Cao, G., Li, H.B., Yin, Z., and Flavell, R.A. (2016). Recent advances in dynamic m^{6}A RNA modification. Open Biol. **6**, 160003.

Cao, X., Jin, X., and Liu, B. (2020). The involvement of stress granules in aging and aging-associated diseases. Aging Cell **19**, e13136.

Chen, H., Yu, Y., Yang, M., Huang, H., Ma, S., Hu, J., Xi, Z., Guo, H., Yao, G., Yang, L., et al. (2022). YTHDF1 promotes breast cancer progression by facilitating FOXM1 translation in an m^{6}A-dependent manner. Cell Biosci. **12**:19.

Doi, K., Izawa, T., Fuse, T., Yamanouchi, U., Kubo, T., Shimatani, Z., Yano, M., and Yoshimura, A. (2004). *Ehd1*, a B-type response regulator in rice, confers short-day promotion of flowering and controls FT-like gene expression independently of *Hd1*. Genes Dev. **18**:926–936.

Dominissini, D., Moshitch-Moshkovitz, S., Salmon-Divon, M., Amariglio, N., and Rechavi, G. (2013). Transcriptome-wide mapping of *N*^{6}-methyladenosine by m^{6}A-seq based on immunocapturing and massively parallel sequencing. Nat. Protoc. **8**:176–189.

Du, H., Zhao, Y., He, J., Zhang, Y., Xi, H., Liu, M., Ma, J., and Wu, L. (2016). YTHDF2 destabilizes m^{6}A-containing RNA through direct recruitment of the CCR4-NOT deadenylase complex. Nat. Commun. **7**, 12626.

Erickson, S.L., and Lykke-Andersen, J. (2011). Cytoplasmic mRNP granules at a glance. J. Cell Sci. **124**:293–297.

Fang, X., Wang, L., Ishikawa, R., Li, Y., Fiedler, M., Liu, F., Calder, G., Rowan, B., Weigel, D., Li, P., and Dean, C. (2019). *Arabidopsis* FLL2 promotes liquid-liquid phase separation of polyadenylation complexes. Nature **569**:265–269.

Fekih, R., Takagi, H., Tamiru, M., Abe, A., Natsume, S., Yaegashi, H., Sharma, S., Sharma, S., Kanzaki, H., Matsumura, H., et al. (2013). MutMap+: Genetic mapping and mutant identification without crossing in rice. PLoS One **8**, e68529.

Foley, J.A., Ramankutty, N., Brauman, K.A., Cassidy, E.S., Gerber, J.S., Johnston, M., Mueller, N.D., O'Connell, C., Ray, D.K., West, P.C., et al. (2011). Solutions for a cultivated planet. Nature **478**:337–342.

Fu, Y., and Zhuang, X. (2020). m^{6}A-binding YTHDF proteins promote stress granule formation. Nat. Chem. Biol. **16**:955–963.

Gao, H., Jin, M., Zheng, X.M., Chen, J., Yuan, D., Xin, Y., Wang, M., Huang, D., Zhang, Z., Zhou, K., et al. (2014). *Days to heading 7*, a major quantitative locus determining photoperiod sensitivity and regional adaptation in rice. Proc. Natl. Acad. Sci. USA **111**:16337–16342.

Gao, H., Zheng, X.M., Fei, G., Chen, J., Jin, M., Ren, Y., Wu, W., Zhou, K., Sheng, P., Zhou, F., et al. (2013). *Ehd4* encodes a novel and *Oryza*-genus-specific regulator of photoperiodic flowering in rice. PLoS Genet. **9**, e1003281.

Ivanov, P., Kedersha, N., and Anderson, P. (2019). Stress granules and processing bodies in translational control. Cold Spring Harbor Perspect. Biol. **11**:a032813.

Iwasaki, S., Takeda, A., Motose, H., and Watanabe, Y. (2007). Characterization of *Arabidopsis* decapping proteins AtDCP1 and AtDCP2, which are essential for post-embryonic development. FEBS Lett. **581**:2455–2459.

Jain, S., Wheeler, J.R., Walters, R.W., Agrawal, A., Barsic, A., and Parker, R. (2016). ATPase-modulated stress granules contain a diverse proteome and substructure. Cell **164**:487–498.

Kasowitz, S.D., Ma, J., Anderson, S.J., Leu, N.A., Xu, Y., Gregory, B.D., Schultz, R.M., and Wang, P.J. (2018). Nuclear m^{6}A reader YTHDC1 regulates alternative polyadenylation and splicing during mouse oocyte development. PLoS Genet. **14**, e1007412.

Kim, D., Langmead, B., and Salzberg, S.L. (2015). HISAT: a fast spliced aligner with low memory requirements. Nat. Methods **12**:357–360.

Kim, S.L., Lee, S., Kim, H.J., Nam, H.G., and An, G. (2007). *OsMADS51* is a short-day flowering promoter that functions upstream of *Ehd1, OsMADS14*, and *Hd3a*. Plant Physiol. **145**:1484–1494.

Kobayashi, K., Yasuno, N., Sato, Y., Yoda, M., Yamazaki, R., Kimizu, M., Yoshida, H., Nagamura, Y., and Kyozuka, J. (2012). Inflorescence meristem identity in rice is specified by overlapping functions of three AP1/FUL-like MADS box genes and PAP2, a SEPALLATA MADS box gene. Plant Cell **24**:1848–1859.

Kojima, S., Takahashi, Y., Kobayashi, Y., Monna, L., Sasaki, T., Araki, T., and Yano, M. (2002). *Hd3a*, a rice ortholog of the *Arabidopsis FT* gene, promotes transition to flowering downstream of *Hd1* under short-day conditions. Plant Cell Physiol. **43**:1096–1105.

Komiya, R., Yokoi, S., and Shimamoto, K. (2009). A gene network for long-day flowering activates RFT1 encoding a mobile flowering signal in rice. Development **136**:3443–3450.

Kosmacz, M., Gorka, M., Schmidt, S., Luzarowski, M., Moreno, J.C., Szlachetko, J., Leniak, E., Sokolowska, E.M., Sofroni, K., Schnittger, A., and Skirycz, A. (2019). Protein and metabolite composition of *Arabidopsis* stress granules. New Phytol. **222**:1420–1433.

Lechler, M.C., Crawford, E.D., Groh, N., Widmaier, K., Jung, R., Kirstein, J., Trinidad, J.C., Burlingame, A.L., and David, D.C. (2017). Reduced Insulin/IGF-1 signaling restores the dynamic properties of key stress granule proteins during aging. Cell Rep. **18**:454–467.

Lee, Y.S., Jeong, D.H., Lee, D.Y., Yi, J., Ryu, C.H., Kim, S.L., Jeong, H.J., Choi, S.C., Jin, P., Yang, J., et al. (2010). *OsCOL4* is a constitutive flowering repressor upstream of *Ehd1* and downstream of *OsphyB*. Plant J. **63**:18–30.

Li, A., Chen, Y.S., Ping, X.L., Yang, X., Xiao, W., Yang, Y., Sun, H.Y., Zhu, Q., Baidya, P., Wang, X., et al. (2017). Cytoplasmic m^{6}A reader YTHDF3 promotes mRNA translation. Cell Res. **27**:444–447.

Li, Y., Wang, X., Li, C., Hu, S., Yu, J., and Song, S. (2014). Transcriptome-wide *N*^{6}-methyladenosine profiling of rice callus and leaf reveals the presence of tissue-specific competitors involved in selective mRNA modification. RNA Biol. **11**:1180–1188.

Liao, S., Sun, H., and Xu, C. (2018). YTH domain: A family of *N*^{6}-methyladenosine (m^{6}A) readers. Dev. Reprod. Biol. **16**:99–107.

Liu, C., Sun, H., Yi, Y., Shen, W., Li, K., Xiao, Y., Li, F., Li, Y., Hou, Y., Lu, B., et al. (2023). Absolute quantification of single-base m^{6}A methylation in the mammalian transcriptome using GLORI. Nat. Biotechnol. **41**:355–366.

Liu, T., Wei, Q., Jin, J., Luo, Q., Liu, Y., Yang, Y., Cheng, C., Li, L., Pi, J., Si, Y., et al. (2020). The m^{6}A reader YTHDF1 promotes ovarian cancer progression via augmenting EIF3C translation. Nucleic Acids Res. **48**:3816–3831.

Lu, S.J., Wei, H., Wang, Y., Wang, H.M., Yang, R.F., Zhang, X.B., and Tu, J.M. (2012). Overexpression of a transcription factor OsMADS15

modifies plant architecture and flowering time in rice (*Oryza sativa* L.). Plant Mol. Biol. Rep. **30**:1461–1469.

Lucas, E., Galán-Martín, Á., Pozo, C., Guo, M., and Guillén-Gosálbez, G. (2021). Global environmental and nutritional assessment of national food supply patterns: Insights from a data envelopment analysis approach. Sci. Total Environ. **755**, 142826.

Lyu, J., Wang, D., Duan, P., Liu, Y., Huang, K., Zeng, D., Zhang, L., Dong, G., Li, Y., Xu, R., et al. (2020). Control of grain size and weight by the GSK2-LARGE1/OML4 pathway in rice. Plant Cell **32**:1905–1918.

Ma, X., Zhang, Q., Zhu, Q., Liu, W., Chen, Y., Qiu, R., Wang, B., Yang, Z., Li, H., Lin, Y., et al. (2015). A robust CRISPR/Cas9 system for convenient, high-efficiency multiplex genome editing in monocot and dicot plants. Mol. Plant **8**:1274–1284.

Matsubara, K., Yamanouchi, U., Nonoue, Y., Sugimoto, K., Wang, Z.X., Minobe, Y., and Yano, M. (2011). *Ehd3*, encoding a plant homeodomain finger-containing protein, is a critical promoter of rice flowering. Plant J. **66**:603–612.

Matsubara, K., Yamanouchi, U., Wang, Z.X., Minobe, Y., Izawa, T., and Yano, M. (2008). *Ehd2*, a rice ortholog of the maize *INDETERMINATE1* gene, promotes flowering by up-regulating *Ehd1*. Plant Physiol. **148**:1425–1435.

Meyer, K.D., Saletore, Y., Zumbo, P., Elemento, O., Mason, C.E., and Jaffrey, S.R. (2012). Comprehensive analysis of mRNA methylation reveals enrichment in 3' UTRs and near stop codons. Cell **149**:1635–1646.

Nemoto, Y., Nonoue, Y., Yano, M., and Izawa, T. (2016). Hd1, a CONSTANS ortholog in rice, functions as an *Ehd1* repressor through interaction with monocot-specific CCT-domain protein Ghd7. Plant J. **86**:221–233.

Patil, D.P., Pickering, B.F., and Jaffrey, S.R. (2018). Reading m^{6}A in the transcriptome: m^{6}A-binding proteins. Trends Cell Biol. **28**:113–127.

Ries, R.J., Zaccara, S., Klein, P., Olarerin-George, A., Namkoong, S., Pickering, B.F., Patil, D.P., Kwak, H., Lee, J.H., and Jaffrey, S.R. (2019). m^{6}A enhances the phase separation potential of mRNA. Nature **571**:424–428.

Riggs, C.L., Kedersha, N., Ivanov, P., and Anderson, P. (2020). Mammalian stress granules and P bodies at a glance. J. Cell Sci. **133**:jcs242487.

Ripin, N., and Parker, R. (2023). Formation, function, and pathology of RNP granules. Cell **186**:4737–4756.

Rosa, S. (2018). Measuring dynamics of histone proteins by photobleaching in *Arabidopsis* roots. Methods Mol. Biol. **1675**:455–465.

Roundtree, I.A., Evans, M.E., Pan, T., and He, C. (2017). Dynamic RNA modifications in gene expression regulation. Cell **169**:1187–1200.

Scutenaire, J., Deragon, J.M., Jean, V., Benhamed, M., Raynaud, C., Favory, J.J., Merret, R., and Bousquet-Antonelli, C. (2018). The YTH domain protein ECT2 is an m^{6}A reader required for normal trichome branching in *Arabidopsis*. Plant Cell **30**:986–1005.

Shao, Y., Wong, C.E., Shen, L., and Yu, H. (2021). *N*^{6}-methyladenosine modification underlies messenger RNA metabolism and plant development. Curr. Opin. Plant Biol. **63**, 102047.

Shi, H., Wang, X., Lu, Z., Zhao, B.S., Ma, H., Hsu, P.J., Liu, C., and He, C. (2017). YTHDF3 facilitates translation and decay of *N*^{6}-methyladenosine-modified RNA. Cell Res. **27**:315–328.

Shi, H., Wei, J., and He, C. (2019). Where, When, and How: Context-Dependent Functions of RNA Methylation Writers, Readers, and Erasers. Mol. Cell **74**:640–650.

Song, P., Yang, J., Wang, C., Lu, Q., Shi, L., Tayier, S., and Jia, G. (2021). *Arabidopsis* *N*^{6}-methyladenosine reader CPSF30-L recognizes FUE signals to control polyadenylation site choice in liquid-like nuclear bodies. Mol. Plant **14**:571–587.

Srikanth, A., and Schmid, M. (2011). Regulation of flowering time: all roads lead to Rome. Cell. Mol. Life Sci. **68**:2013–2037.

Tamaki, S., Matsuo, S., Wong, H.L., Yokoi, S., and Shimamoto, K. (2007). Hd3a protein is a mobile flowering signal in rice. Science **316**:1033–1036.

Taoka, K.i., Ohki, I., Tsuji, H., Furuita, K., Hayashi, K., Yanase, T., Yamaguchi, M., Nakashima, C., Purwestri, Y.A., Tamaki, S., et al. (2011). 14-3-3 proteins act as intracellular receptors for rice Hd3a florigen. Nature **476**:332–335.

Tsuji, H., Nakamura, H., Taoka, K.i., and Shimamoto, K. (2013). Functional diversification of FD transcription factors in rice, components of florigen activation complexes. Plant Cell Physiol. **54**:385–397.

Tsuji, H., Taoka, K.i., and Shimamoto, K. (2011). Regulation of flowering in rice: two florigen genes, a complex gene network, and natural variation. Curr. Opin. Plant Biol. **14**:45–52.

Wang, J., Wang, L., Diao, J., Shi, Y.G., Shi, Y., Ma, H., and Shen, H. (2020a). Binding to m^{6}A RNA promotes YTHDF2-mediated phase separation. Protein Cell **11**:304–307.

Wang, W., Wang, C., Wang, Y., Ma, J., Wang, T., Tao, Z., Liu, P., Li, S., Hu, Y., Gu, A., et al. (2023). The P-body component DECAPPING5 and the floral repressor SISTER OF FCA regulate FLOWERING LOCUS C transcription in *Arabidopsis*. Plant Cell **35**:3303–3324.

Wang, Y., Xiao, Y., Dong, S., Yu, Q., and Jia, G. (2020b). Antibody-free enzyme-assisted chemical approach for detection of *N*^{6}-methyladenosine. Nat. Chem. Biol. **16**:896–903.

Weber, C., Nover, L., and Fauth, M. (2008). Plant stress granules and mRNA processing bodies are distinct from heat stress granules. Plant J. **56**:517–530.

Wei, L.H., Song, P., Wang, Y., Lu, Z., Tang, Q., Yu, Q., Xiao, Y., Zhang, X., Duan, H.C., and Jia, G. (2018). The m^{6}A Reader ECT2 controls trichome morphology by affecting mRNA stability in *Arabidopsis*. Plant Cell **30**:968–985.

Wei, X., Xu, J., Guo, H., Jiang, L., Chen, S., Yu, C., Zhou, Z., Hu, P., Zhai, H., and Wan, J. (2010). *DTH8* suppresses flowering in rice, influencing plant height and yield potential simultaneously. Plant Physiol. **153**:1747–1758.

Wu, X., Su, T., Zhang, S., Zhang, Y., Wong, C.E., Ma, J., Shao, Y., Hua, C., Shen, L., and Yu, H. (2024). *N*^{6}-methyladenosine-mediated feedback regulation of abscisic acid perception via phase-separated ECT8 condensates in *Arabidopsis*. Nat. Plants **10**:469–482.

Xu, J., Yang, J.Y., Niu, Q.W., and Chua, N.H. (2006). *Arabidopsis* DCP2, DCP1, and VARICOSE form a decapping complex required for postembryonic development. Plant Cell **18**:3386–3398.

Xue, W., Xing, Y., Weng, X., Zhao, Y., Tang, W., Wang, L., Zhou, H., Yu, S., Xu, C., Li, X., and Zhang, Q. (2008). Natural variation in *Ghd7* is an important regulator of heading date and yield potential in rice. Nat. Genet. **40**:761–767.

Yano, M., Katayose, Y., Ashikari, M., Yamanouchi, U., Monna, L., Fuse, T., Baba, T., Yamamoto, K., Umehara, Y., Nagamura, Y., and Sasaki, T. (2000). *Hd1*, a major photoperiod sensitivity quantitative trait locus in rice, is closely related to the *Arabidopsis* flowering time gene *CONSTANS*. Plant Cell **12**:2473–2484.

Youn, J.Y., Dyakov, B.J.A., Zhang, J., Knight, J.D.R., Vernon, R.M., Forman-Kay, J.D., and Gingras, A.C. (2019). Properties of stress granule and P-body proteomes. Mol. Cell **76**:286–294.

Zhang, Y., Su, J., Duan, S., Ao, Y., Dai, J., Liu, J., Wang, P., Li, Y., Liu, B., Feng, D., et al. (2011). A highly efficient rice green tissue protoplast system for transient gene expression and studying light/chloroplast-related processes. Plant Methods **7**:30.

Zhang, Z., Luo, K., Zou, Z., Qiu, M., Tian, J., Sieh, L., Shi, H., Zou, Y., Wang, G., Morrison, J., et al. (2020). Genetic analyses support the contribution of mRNA N^6-methyladenosine (m^{6}A) modification to human disease heritability. Nat. Genet. **52**:939–949.

Zhao, B.S., Roundtree, I.A., and He, C. (2017). Post-transcriptional gene regulation by mRNA modifications. Nat. Rev. Mol. Cell Biol. **18**:31–42.

Zhou, L., Gao, G., Tang, R., Wang, W., Wang, Y., Tian, S., and Qin, G. (2022). m^{6}A-mediated regulation of crop development and stress responses. Plant Biotechnol. J. **20**:1447–1455.